3×10^4 cells/well in a 24-well culture dish and were transfected with 40 ng of NF-κB reporter plasmid (pNF-κB-Luc; BD Biosciences/BD Clontech), 2 ng of *NEMO* mutant expression construct, 10 ng of internal control for the normalization of transfection efficiency (pRL-TK; Toyo Ink), and 148 ng of mock vector using FuGENE HD Transfection Reagent (TOYO-B-Net) according to the manufacturer's protocol. Twelve hours after transfection, the cells were stimulated with 15 ng/mL lipopolysaccharide (LPS; Sigma-Aldrich) for 4 hours and the NF-κB activity was measured using the PicaGene Dual SeaPansy assay kit (TOYO-B-Net). Experiments were performed in triplicate and firefly luciferase activity was normalized to *Renilla* luciferase activity.

Subcloning analysis of cDNA

Cell sorting of the various cell lineages was performed by FACSVantage (BD Biosciences). The purity of each lineage was > 95%. The cDNA from sorted cells was purified and reverse transcribed by Super Script III (Invitrogen) with random hexamers and amplified by the proofreading PCR enzyme KOD, as previously described.[17,21] The PCR primers used were NEMO2 (5′-AGAGACGAAGGAGCACAAAGCTGCCTTGAG-3′) and NEMO3 (5′-ACTGCAGGGACAATGGTGGGTGCATCTGTC-3′). The PCR products were subcloned using a TA cloning kit (Invitrogen) and sequenced by ABI 3130xl Genetic analyzer (Applied Biosystems). To determine whether additional mutations occurred in revertant subclones that had wild-type sequence in the original mutation site, the entire coding region of the *NEMO* gene was sequenced and an additional mutation was considered present when the same mutation was detected in multiple subclones.

Allele-specific PCR

The mRNA purified from sorted T cells and monocytes was reverse-transcribed by SuperScript III (Invitrogen) with the gene-specific primer NEMO2 and amplified by the proofreading PCR enzyme KOD (Toyobo) using the primers NEMO3 and NEMO 4 (5′-TGTGGACACGCAGTGAAACGTGGTCTGGAG-3′). The PCR products were used as templates for allele-specific PCRs with Ex Taq polymerase (Takara Bio). Mutant and wild-type *NEMO* DNA was generated from each NEMO expression plasmid, mixed at graded ratios, and used as controls. PCR conditions and primer sequences are listed in supplemental Table 1 (available on the *Blood* Web site; see the Supplemental Materials link at the top of the online article).

Proliferation of NEMO^{normal} and NEMO^{low} T cells

To obtain PHA-induced T-cell blasts, PBMCs were stimulated with PHA (1:100; Invitrogen) and cultured in RPMI 1640 supplemented with 5% FCS and recombinant human IL-2 (50 IU/mL; kindly provided by Takeda Pharmaceutical Company) at 37°C for 7 days. Subcloning analysis of the cDNA obtained from the T-cell blasts was performed as described in "Subcloning analysis of cDNA."

Results

Reversion mosaicism of NEMO occurred in siblings with similar immunologic phenotypes

We previously reported patient 1 with a duplication mutation of the *NEMO* gene spanning intron 3 to exon 6, who was diagnosed as XL-EDA-ID at 1 year of age after suffering from recurrent infections.[17] At first, genetic diagnosis of the patient was difficult because the expression of aberrant *NEMO* mRNA was masked by the expression of normal *NEMO* mRNA by the revertant cells. Flow cytometric analysis of intracellular NEMO expression revealed cells with normal (NEMO^{normal}) and reduced (NEMO^{low}) levels of NEMO expression, indicating the presence of reversion mosaicism of the *NEMO* gene, and further analysis revealed that the *NEMO* mutation was disease-causing. PCR across the mutated region and sequencing of the PCR products revealed a duplication extending from intron 3 to exon 6, which was confirmed by Southern blot analysis. Additional copy number analysis of the *NEMO* gene of patient 1 and his mother excluded the possibility of a complex chromosomal aberration such as multiple duplication of the *NEMO* gene (supplemental Figure 1). Furthermore, polymorphism analysis using variable number tandem repeats on NEMO^{normal} and NEMO^{low} cells from patient 1 revealed that these cells were derived from the same origin (supplemental Table 2), indicating that the *NEMO* gene mosaicism was less likely because of amalgamation. The genomic analysis of the NEMO^{normal} cells revealed a complete reversion of the *NEMO* gene with no additional mutations. The clinical phenotype of patient 1 was combined immunodeficiency with a reduced number of T cells and mitogen-induced proliferation (Tables 2-3). We previously determined that reduced NEMO expression in the mutant T cells caused impairment of T-cell development and mitogen-induced proliferation.

Patient 2, the younger brother of patient 1, was diagnosed as XL-EDA-ID with the same duplication mutation as his brother. Flow cytometric analysis of intracellular NEMO expression performed at diagnosis showed that most of his PBMCs had reduced NEMO expression (Figure 1A). At 2 months of age, when most of the T cells were NEMO^{low}, absolute counts of the patient's T cells and the mitogen-induced proliferation of the patient's PBMCs were comparable with those of the healthy controls (Figure 1A-B; Table 2). These findings indicated that the *NEMO* mutation had no effect on T-cell development and mitogen-induced proliferation during early infancy in patient 2.

NEMO^{normal} T cells gradually increased as patient 2 grew older, while the absolute count of NEMO^{low} T cells decreased (Figure 1A-B). Accordingly, normal full-length *NEMO* cDNA, which had been undetectable in cord blood, was detectable in the patient's peripheral blood at 12 months of age. However, while NEMO^{normal} T cells were increasing, mitogen-induced T-cell proliferation started to decrease (Table 3), and the patient started to show poor weight gain from 6 months of age. When patient 2 was 17 months old, a blood culture revealed an *M szulgai* bacteremia. At this time, the absolute count of NEMO^{normal} T cells peaked, and NEMO^{low} T cells were at a minimum. He began to gain weight after anti-*Mycobacterium* medication was initiated, although NEMO^{normal} T cells started to decrease and NEMO^{low} T cells began to increase (Figure 1B). When the patient was 23 months old, mitogen-induced T-cell proliferation was still low and a roughly equal number of NEMO^{low} and NEMO^{normal} T cells were detected (Table 3). Overall, as patient 2 grew older, NEMO^{normal} T cells increased as the total number of T cells and the mitogen-induced T-cell proliferation decreased, similar to what had occurred in patient 1 at a similar age.

Various analyses were performed to compare the immunologic phenotype of NEMO^{low} and NEMO^{normal} T cells in detail. Both NEMO^{normal} and NEMO^{low} CD4$^+$ T cells carried a diverse Vβ repertoire, but CD8$^+$ T cells had a skewed Vβ repertoire regardless of NEMO expression level (Figure 1C). Surface marker analysis revealed that most of the NEMO^{normal} T cells were CD45RA$^-$/CCR7$^-$ and most of the NEMO^{low} T cells were CD45RA$^+$/CCR7$^+$ (Figure 1D). The NEMO^{normal} T cells produced similar amounts of IFN-γ and TNF-α as healthy control cells, while the production of these cytokines were reduced in NEMO^{low} T cells (Figure 1E-F). Taken together, these data implied that the immunologic phenotype of T cells from patient 2 converged with that of patient 1 as patient 2 grew older.

Table 2. Surface marker analysis of peripheral mononuclear cells of patients 1 and 2

	Patient 1	Patient 2		Healthy controls
Age at analysis	2 y	2 mo	19 mo	
CD3	1503	2366	1014	2997 ± 1751
CD4	292	1583	374	1683 ± 874
CD8	1160	783	547	1114 ± 976
TCRαβ	1386	2295	439	2620 ± 1612
TCRγδ	109	74	574	343 ± 177
CD4$^+$CD45RA	58	1336	105	1471 ± 890
CD4$^+$CD45RO	263	307	266	497 ± 189
CD8$^+$CD45RA	1178	783	297	1083 ± 1078
CD8$^+$CD45RO	361	21	250	385 ± 442
CD4$^+$CD25	80	427	93	210 ± 99
CD19	1200	941	1543	1252 ± 1145
CD20	1189	931	1536	1125 ± 837
CD19$^+$Sm-IgG	7	18	17	54 ± 21
CD19$^+$Sm-IgA	15	4	14	18 ± 14
CD19$^+$Sm-IgM	1171	910	1505	1057 ± 881
CD19$^+$Sm-IgD	1171	906	1495	1052 ± 884
CD16	912	176	24	287 ± 200
CD56	908	176	24	306 ± 207

Surface markers expressed by XL-EDA-ID patients' PBMCs are shown as absolute counts per microliter of peripheral blood. Healthy control values are based on children aged 1 to 6 years and are shown as the mean ± SD.

Sm indicates the surface membrane.

High incidence of somatic mosaicism of the *NEMO* gene in XL-EDA-ID patients

It is worth noting that somatic reversion mosaicism of the *NEMO* gene occurred in both of the 2 XL-EDA-ID siblings carrying a duplication mutation. To determine whether a high frequency of reversion is a specific event for this type of *NEMO* duplication mutation[22-25] or if the reversion of the *NEMO* gene occurs commonly in XL-EDA-ID patients, we recruited an additional 8 XL-EDA-ID patients from throughout Japan (Table 1) and analyzed the presence of *NEMO* reversion. These patients had various combinations of clinical phenotypes characteristic of XL-EDA-ID such as ectodermal dysplasia, innate and acquired immunity defects, and susceptibility to pyogenic bacteria and *Mycobacterium* infections. Every patient had a mutation of the *NEMO* gene with reduced NF-κB activation potential, as evaluated in a NEMO reconstitution assay (Figure 2).

Among the 8 patients, only patient 3 had a large proportion of NEMO^{low} cells by flow cytometric analysis. The majority of patient 3's PBMCs were NEMO^{low}, whereas 10% of the patient's CD8$^+$ cells were NEMO^{normal} (Figure 3A). This patient was identified as carrying the D311E mutation. Because missense mutations of the *NEMO* gene often do not result in the reduced expression of NEMO protein, subcloning and sequencing analysis was performed on the *NEMO* cDNA isolated from the remaining patients, and 6 of the 7 patients had normal *NEMO* subclones (Table 3). Expansion of maternal cells after fetomaternal transfusion was ruled out in these patients by FISH analysis with X and Y probes (Table 1).

Additional genetic analysis of the entire coding region of the *NEMO* gene was performed on NEMO^{normal} cells from patient 3 and on reverted subclones from the other patients, except for patient 10 who had already received stem cell transplantation. The *NEMO* gene in these samples had reverted to wild-type with no additional mutations (Figure 3B and data not shown). To specifically determine in which cell lineages the reversion occurred, subcloning and sequencing analysis of cDNA in various cell lineages was performed. This analysis revealed that all the revertant cells were of the T-cell lineage and that no reversion occurred in monocytes and very little occurred in B cells (Table 4). Allele-specific PCR confirmed that reversion occurred in T cells but not in monocytes (Figure 4).

Selective advantage of NEMO^{normal} cells in XL-EDA-ID carriers

The high frequency of somatic mosaicism in T cells of XL-EDA-ID patients indicated a strong selective advantage of wild-type NEMO T cells over T cells carrying mutant NEMO. To confirm this hypothesis, *NEMO* cDNA analysis was performed on various cell lineages from the mothers of the patients who are heterozygous for *NEMO* mutation and thus have mosaicism

Table 3. Immunologic analysis of patients 1 and 2

	Patient 1	Patient 2 (treated with IVIG)	
Age at analysis, mo	9	9	20
Serum immunoglobulin levels, g/L (control)			
IgG	10.63 (4.51-10.46)	8.44 (4.51-10.46)	10.37 (7.15-9.07)
IgA	1.36 (0.14-0.64)	1.88 (0.14-0.64)	3.93 (0.22-1.44)
IgM	0.4 (0.33-1.00)	0.17 (0.33-1.00)	0.20 (0.34-1.28)
Age at analysis	2 y	2 mo	23 mo
T-cell proliferation, SI (control)	9.3 (206.9 ± 142.5)	55.3 (64.8 ± 8.1)	7.2 (89.4 ± 31.2)

Control values of serum immunoglobulin levels are based on children aged either 7 to 9 months or 1 to 2 years and are shown as the mean ± SD. The T-cell proliferation assay was performed as described previously[17] with at least three healthy adults as controls.

SI indicates stimulation index; and IVIG, 2.5 g of monthly IV immune globulin infusion.

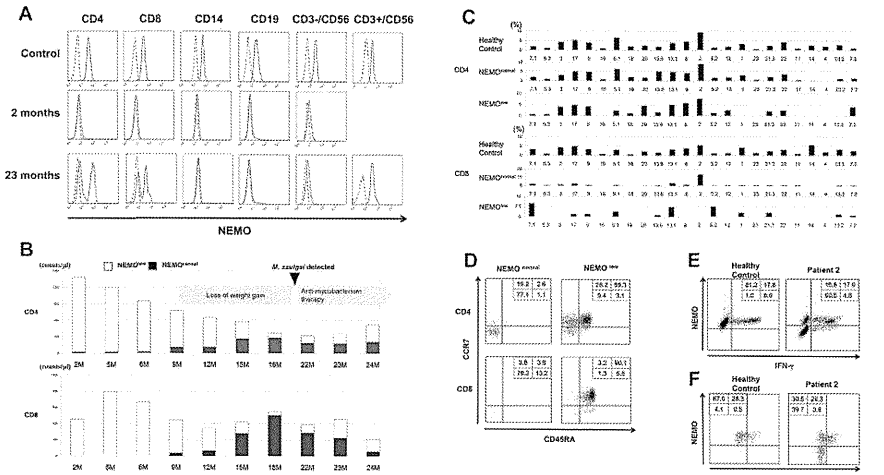

Figure 1. Identification and characterization of *NEMO* revertant T cells in patient 2. (A) Intracellular expression of NEMO in various PBMC lineages from a healthy adult control and patient 2 were evaluated by flow cytometry. For the patient, results of the analyses performed at 2 months and 23 months are shown. Solid lines indicate staining with the anti-NEMO mAb, and dotted lines indicate the isotype control. (B) Time-course variations in the absolute count of NEMO^{normal} and NEMO^{low} T cells in patient 2. M indicates age in months. (C) TCR-Vβ repertoire analysis of the patient's CD4$^+$ and CD8$^+$ T cells. PBMCs from the patient and a healthy adult control were stained for the TCR-Vβ panel, CD4, CD8, and NEMO, and analyzed by flow cytometry. (D) Phenotype analysis of T cells in patient 2. PBMCs from the patient and a control were stained for the expression of NEMO, CCR7, CD45RA, and CD4 or CD8. Data shown were gated on NEMO^{normal} or NEMO^{low} CD4$^+$ or CD8$^+$ cells. (E-F) Cytokine production from NEMO^{normal} and NEMO^{low} T cells. PBMCs from the patient and a control were stimulated with PMA and ionomycin for 6 hours and stained for intracellular (E) IFN-γ or (F) TNF-α along with NEMO. Cells shown are gated on the CD3$^+$ population.

because of X-chromosome inactivation. This analysis assumes that the percentage of cDNA for wild-type *NEMO* reflects the percentage of cells expressing wild-type NEMO. A high proportion of wild-type *NEMO* cDNA was observed in T cells from the mothers of patients 1/2, 3, 8, and 10, although wild-type *NEMO* cDNA was not predominant in T cells from the mother of patient 4 (Table 5).

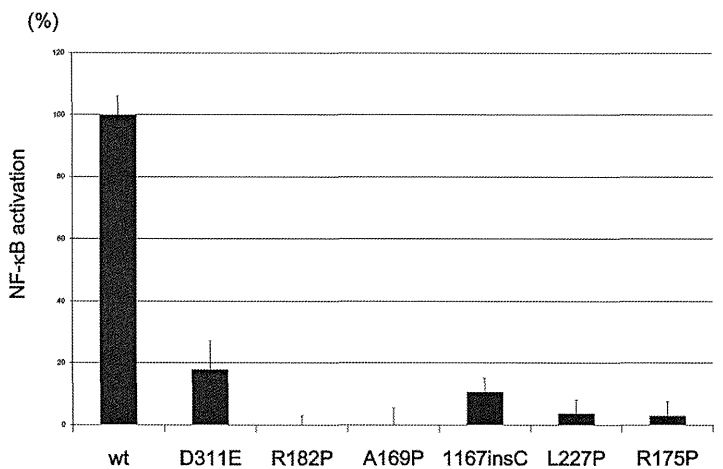

Figure 2. NF-κB transactivation by NEMO mutants from the XL-EDA-ID patients. NF-κB transactivation induced by NEMO mutants in the XL-EDA-ID patients. Mock vectors and wild-type (wt) NEMO were used as controls. The NF-κB activation index of NEMO variants were calculated as (NF-κB activation by each NEMO variant − NF-κB activation of the mock vector)/(NF-κB activation by wild-type NEMO − NF-κB activation of the mock vector). The data shown are the mean ± SD of triplicate wells and are representative of 3 independent experiments with similar results.

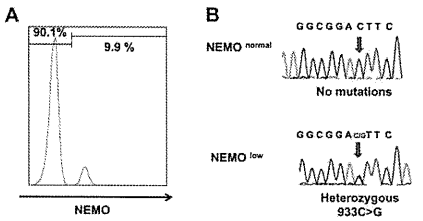

Figure 3. *NEMO* revertant T cells in patient 3. (A) Intracellular expression of NEMO in CD8$^+$ cells from patient 3. (B) Sequencing chromatograms of DNA from NEMO^{normal} or NEMO^{low} CD8$^+$ cells of patient 3. Arrows indicate the mutated base position at c. 931.

Similarly, there was an apparent high proportion of wild-type *NEMO* cDNA in monocytes and B cells from the mothers of patients 1/2, 8, and 10 (Table 5). These findings suggested a general selective advantage of NEMO^{normal} cells over NEMO^{low} cells in vivo, especially in T cells.

Proliferation capacity of NEMO^{normal} and NEMO^{low} T cells

T-cell proliferation stimulated by mitogens such as PHA is usually not reduced in XL-EDA-ID patients. However, the emergence of NEMO^{normal} cells coincided with a reduction in mitogen-induced proliferation in patient 2. To further determine the effect of NEMO^{normal} cells on mitogen-induced proliferation of peripheral T cells, the proportions of T cells carrying the wild-type and mutant were examined before and after PHA stimulation in XL-EDA-ID patients and their mothers (Table 6). In patients 2, 4, and 8, the percentage of the NEMO^{normal} cells decreased after PHA stimulation, while NEMO^{normal} cells prevailed in patient 9. In the mothers of patient 4 and 10, the percentage of NEMO^{normal} cells increased after PHA stimulation, while the percentage of the NEMO^{normal} cells decreased in the mother of patient 3. These results indicated that the NEMO mutation does not directly affect the mitogen-induced proliferation capacity of T cells and factors other than the *NEMO* genotype determine the proliferation capacity of NEMO^{normal} and NEMO^{low} T cells.

Discussion

Somatic reversion mosaicism has been described in several disorders affecting the hematopoietic system, the liver, and the skin.[23,26] Reports of somatic reversion cases have been particularly abundant in patients with immunodeficiency diseases, including Wiskott-Aldrich syndrome (WAS)[27] and SCID, which occur because of mutations in the interleukin receptor common γ chain,[28] CD3ζ,[29] *RAG-1*[30], and *ADA* genes.[31] Patients with somatic reversion mosaicism may present with significantly milder clinical phenotypes compared with nonrevertant patients with the same germline mutation, although this is not always the case.[26] One common feature in most cases where the somatic reversion mosaicism has been observed is a strong in vivo selective advantage of the revertant cells that express the wild-type gene product. One of the most intensively investigated diseases associated with somatic reversion mosaicism is WAS.[32-34] A report showed that up to 11% of WAS patients have presented with somatic reversion mosaicism.[33]

In our investigation, 9 of 10 XL-EDA-ID patients presented with somatic mosaicism. Two of the 9 were cases of reversion from a duplication mutation, while the others exhibited true back-reversion from a substitution or insertion mutation. This finding calls for caution when diagnosing XL-EDA-ID patients. Because the existence of a *NEMO* pseudogene makes it difficult to perform genetic analysis using genomic DNA, diagnosis of the disease is often confirmed by sequencing analysis of *NEMO* cDNA, and the presence of somatic mosaicism can cause misdiagnosis of XL-EDA-ID patients either when NEMO^{normal} cells make up the majority of the patients' PBMCs or when the cDNA of the mutated *NEMO* gene cannot be amplified by PCR.[17] In fact, mutated *NEMO* cDNA could not be amplified from the PBMCs of patient 2 even when NEMO^{normal} cells were absent (during early infancy), and only wild-type *NEMO* cDNA was amplified after the appearance of NEMO^{normal} cells (data not shown), probably because of the instability of the mutated *NEMO* mRNA. Flow cytometric analysis of intracellular NEMO protein is of help in identifying the NEMO^{low} cells in some patients, but the technique is not applicable when the *NEMO* mutation does not cause reduced expression of NEMO protein. Thus, some cases of XL-EDA-ID patients with reversion may be difficult to diagnose.

The high frequency of somatic mosaicism observed in XL-EDA-ID patients indicates a strong in vivo selective advantage for NEMO^{normal} cells, which express the wild-type gene product. Patient 2 presented with a high mutant T-cell count at birth that gradually decreased over time (Figure 1B). This finding indicates that wild-type NEMO expression is critical for the survival of certain cell lineages, including T cells, after birth. On the other hand, no NEMO^{normal} monocytes and very few NEMO^{normal} B cells were detected in the recruited XL-EDA-ID patients (Table 4). This specific feature is similar to other somatic reversion mosaicism seen in primary immunodeficiency patients[26] and indicates that the expression of NEMO is less critical for the survival of monocytes or B cells compared with that of T cells. There is also an apparent

Table 4. Analysis of *NEMO* gene mosaicism in various cell lineages for each patient

Patient	Mutation	Age at analysis	CD4, % (proportion)	CD8, % (proportion)	CD14, % (proportion)	CD19, % (proportion)
1	Duplication	2 y	90	100	0	4.0
2	Duplication	15 mo	45	66	0	4.0
3	D311E	3 y	2.4	9.9	0	1.2
4	A169P	12 y	0 (0/19)	24 (9/37)	0 (0/19)	0 (0/47)
5	L227P	3 y	0 (0/25)	0 (0/35)	0 (0/30)	0 (0/25)
6	R182P	4 y	18 (5/28)	17 (9/52)	0 (0/27)	0 (0/33)
7	R175P	6 y	0.4 (1/25)	39 (11/28)	0 (0/28)	0 (0/25)
8	Q348X	8 y	38 (6/16)	47 (9/19)	0 (0/33)	0 (0/25)
9	R175P	15 y	30 (9/30)	36 (12/33)	0 (0/23)	0 (0/14)
10	1167 ins C	9 mo	PBMC 9.3 (4/43)			

For patients 1 to 3, data represent the percentages of NEMO^{normal} cells in each lineage, as assessed by flow cytometry. For patients 4 to 10, the ratio indicates the number of wild-type NEMO clones in various cell lineages as compared with the total number of clones analyzed, based on subcloning and sequencing analysis.

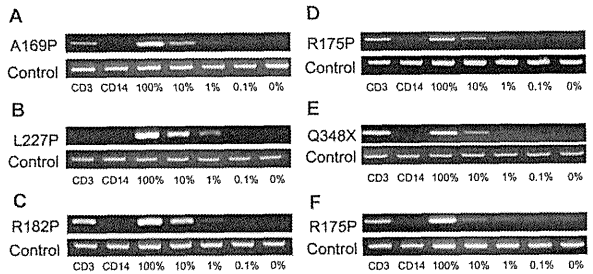

Figure 4. NEMO reversion selectively occurs in T cells of XL-EDA-ID patients. Allele-specific PCR for *NEMO* on CD3+ or CD14+ cells from (A) patient 4, (B) patient 5, (C) patient 6, (D) patient 7, (E) patient 8, and (F) patient 9. Numbers below each figure indicate the percentages of wild-type NEMO cDNA mixed with each mutant. Primers used in each PCR are shown on the left.

concordance between the degree of the disruption of *NEMO* gene and the proportion of reverted NEMO^{normal} cells compared with NEMO^{low} cells. The high proportion of reverted T cells seen in patients 1 and 2 as well as in patient 8 was associated with a highly disruptive mutation of the *NEMO* gene (ie, a duplication mutation in patients 1 and 2, and a truncation mutation in patient 8). In addition, the highly selective X-chromosome inactivation observed in the mothers of XL-EDA-ID patients indicated a strong selective advantage for NEMO^{normal} cells over NEMO^{low} cells. It is also noteworthy that reverted T cells were not detected in patient 5, who carried an L227P mutation that was not localized to either of the functional domains in the NEMO protein. Other reported cases with the same mutation presented with polysaccharide-specific humoral immunodeficiency and autoinflammatory diseases, but were spared complications such as cellular immunodeficiency and susceptibility to *Mycobacterium* (similar to patient 5).[4,8] This may reflect the fact that the L227P mutation in NEMO has less influence on T-cell growth than NEMO mutations that occur in functional domains, and suggests that reversion of the mutation has little impact on T-cell survival. Although the number of cases in our study is limited, it appears that the more disruptive NEMO mutations favor the survival of NEMO^{normal} cells after reversion and X-chromosome inactivation.

Regarding the gradual decline in the number of NEMO-deficient T cells, one candidate trigger could be infection. Because the dominance of the memory phenotype and the skewed TCR repertoire among CD8+ T cells in NEMO^{normal} cells were observed in both patients 1 and 2 (Figure 1C and Mizukami et al[18]), continuous infection of pyogenic bacteria in patient 1 and *M szulgai* in patient 2 could be a reason for the emergence of NEMO^{normal} cells and the elimination of NEMO^{low} cells. The decrease in NEMO^{normal} cells and restoration of NEMO^{low} cells after anti-mycobacterial therapy in patient 2 support this hypothesis. In the case of patient 1, the predominance of NEMO^{normal} T cells with an effector/memory phenotype at diagnosis (Table 4 and Mizukami et al[18]) is likely to be the result of chronic infection, and it is possible that NEMO^{low} cells were predominant during his early infancy. Because some reports have indicated that TNF-α–induced programmed cell death of several cell types, including a human T-cell line, was enhanced by hypomorphic *NEMO* mutations,[12,35] and considering our finding that the levels of TNF-α expressed in revertant T cells were similar to levels in healthy control T cells in vitro (Figure 1F), TNF-α produced from these cells in response to infection could be involved in mutant T-cell elimination.

Unexpectedly, T-cell proliferation in patient 2 was equivalent to that of normal controls at the age of 2 months and was reduced after NEMO^{normal} T cells increased (Figure 1B; Table 3). This finding indicates that the NEMO^{low} T cells did not have intrinsically impaired mitogen-induced proliferation. One reasonable explanation for the reduced proliferation observed after the increase in NEMO^{normal} T cells is a reduction in the absolute number of T cells (naive T cells in particular), probably because of the infection.

Table 5. Expression of mutant NEMO in various cell lineages for the mother of each XL-EDA-ID patient

Sample	Mutation	Analysis	Subtype	Mutant type, % (proportion)
Mother of patients 1 and 2	Duplication	FACS	CD3	0
			CD14	0
			CD19	0
Mother of patient 3	D311E	FACS	CD3	13
			CD3$^-$	54
		Subcloning	CD3	22 (6/27)
			CD3$^-$	55 (12/22)
Mother of patient 4	A169P	Subcloning	CD3	52 (11/21)
			CD14	58 (11/19)
			CD19	42 (5/12)
Mother of patient 8	Q348X	Subcloning	CD3	0 (0/26)
			CD14	17 (3/18)
			CD19	0 (0/18)
Mother of patient 10	1167insC	Subcloning	CD3	18 (7/39)
			CD14	12 (5/43)
			CD19	27 (12/44)

Data are shown as either the percentages of NEMO^{normal} cells, as assessed by flow cytometry, or as the ratio of clones containing wild-type NEMO to the total number of clones, as analyzed by subcloning and sequencing analysis.

Table 6. Expression of mutant NEMO in CD3-positive cells and PHA blasts

Sample	Mutations	Analysis	Subtype	Mutant type, % (proportion)
Mother of patient 3	D311E	FACS	CD3	13
			PHA blast	47
		Subcloning	CD3	22 (6/27)
			PHA blast	48 (11/23)
Mother of patient 4	A169P	Subcloning	CD3	52 (11/21)
			PHA blast	18 (9/49)
Mother of patient 8	Q348X	Subcloning	CD3	0 (0/26)
			PHA blast	0 (0/21)
Mother of patient 10	1167insC	Subcloning	CD3	18 (7/39)
			PHA blast	9 (4/43)
Patient 2	Duplication	FACS	CD3	73
			PHA blast	93
Patient 4	A169P	Subcloning	CD3	79 (19/24)
			PHA blast	100 (37/37)
Patient 8	Q348X	Subcloning	CD3	56 (18/32)
			PHA blast	100 (16/16)
Patient 9	R175P	Subcloning	CD3	87 (34/39)
			PHA blast	0 (0/28)

PHA blasts were obtained by incubating PBMCs with PHA and soluble IL-2 for 7 days. Data are shown as either the percentages of NEMO^{normal} cells, as assessed by flow cytometry, or as the ratio of clones containing wild-type NEMO to the total number of clones, as analyzed by subcloning and sequencing analysis.

Therefore, to identify other mechanisms underlying reduced T-cell proliferation, the impact of *NEMO* mutation on PHA-induced T-cell proliferation was indirectly examined in vitro by comparing the response of NEMO^{normal} and NEMO^{low} cells derived from XL-EDA-ID patients and their mothers. After PHA stimulation and proliferation, the proportion of NEMO^{low} T cells increased in patients 2, 4, and 8, while the opposite result was observed in patient 9 and in the mother of patient 4 (Table 6). Although the precise mechanism is unclear, a reduction in the proportion of NEMO^{normal} cells after PHA stimulation would reflect the lower proliferative capacity of NEMO^{normal} cells compared with that of NEMO^{low} cells, which may be another explanation for the reduced T-cell proliferation observed in patient 2 at 23 months of age when NEMO^{normal} T cells were dominant. In the reports on reversion mosaicism of *IL2RG* gene mutations,[28,36] the restoration of T-cell function and clinical symptoms varied among patients. Therefore, other factors besides the genotype of the mutations, such as the developmental stage where reversion occurred and the frequency of reversion, affect the clinical impact of somatic mosaicism of *NEMO* gene mutations.

In this study, the effect of somatic mosaicism of the *NEMO* gene on clinical phenotype could not be fully evaluated. However, cytokines produced by revertant T cells could influence the development of clinical symptoms of XL-EDA-ID, such as inflammatory bowel disease. In a mouse model, intestinal epithelial cell-specific inhibition of NF-κB through the conditional ablation of NEMO resulted in the development of chronic bowel inflammation sensitized intestinal epithelial cells to TNF-α–induced apoptosis.[37] In this model, the first phase of intestinal inflammation was initiated by epithelial cell death and was followed by a second phase of TNF-α–induced intestinal inflammation, the latter being dependent on T cells. Another report showed that HSCT in XL-EDA-ID patients exacerbated the patients' inflammatory bowel disease.[38] Indeed, in patient 4, the percentage of reverted T cells was reduced after repeated administrations of anti-TNFα blocking Ab, and the symptoms of inflammatory bowel disease improved.[18] Considering this evidence, somatic mosaicism in T cells might be an important factor leading to inflammatory disease in XL-EDA-ID patients with defective NF-κB activation. However, our study did not show a tight association between inflammatory bowel disease and somatic mosaicism, and further investigation is needed to determine whether the NEMO^{normal} T cells play a role in inflammatory processes in XL-EDA-ID.

In conclusion, this study has identified a high frequency of somatic mosaicism in XL-EDA-ID patients, particularly in T cells, and has revealed important insights into human T-cell immunobiology in XL-EDA-ID. Although we could not demonstrate the clinical impact of somatic mosaicism in XL-EDA-ID patients, our findings suggest that care is required when making molecular diagnoses of XL-EDA-ID, and might shed light on the mechanisms underlying the variability in the clinical manifestation of XL-ED-ID and facilitate the search for appropriate treatments.

Acknowledgments

The authors are grateful to all the XL-EDA-ID patients and their families for their participation. They also thank Shoji Yamaoka (Department of Molecular Virology, Graduate School of Medicine, Tokyo Medical and Dental University, Tokyo, Japan) for kindly providing NEMO-null rat fibroblast cells, and Takeda Pharmaceutical Company Limited for kindly providing the recombinant human IL-2.

This work was supported by grants from the Japanese Ministry of Education, Culture, Sports, Science, and Technology, and by grants from the Japanese Ministry of Health, Labor and Welfare.

Authorship

Contribution: Tomoki Kawai wrote the manuscript and performed research; R.N., T.Y., T.N., and T.H. edited the manuscript and supervised this work; K.I., Y.M., N.T., H.S., M.S., and Y.T. cultured cells; and T. Mizukami, H.N., Y.K., A.Y., T. Murata, S.S., E.I., H.A., Toshinao Kawai, C.I., S.O., and M.K. treated patients and analyzed data.

Conflict-of-interest disclosure: The authors declare no competing financial interests.

Correspondence: Ryuta Nishikomori, MD, PhD, Department of Pediatrics, Kyoto University Graduate School of Medicine, 54 Kawahara-cho, Shogoin, Sakyo-ku, Kyoto 606-8507, Japan; e-mail: rnishiko@kuhp.kyoto-u.ac.jp.

References

1. Pinheiro M, Freire-Maia N. Ectodermal dysplasias: a clinical classification and a causal review. *Am J Med Genet.* 1994;53(2):153-162.
2. Abinun M, Spickett G, Appleton AL, Flood T, Cant AJ. Anhidrotic ectodermal dysplasia associated with specific antibody deficiency. *Eur J Pediatr.* 1996;155(2):146-147.
3. Sitton JE, Reimund EL. Extramedullary hematopoiesis of the cranial dura and anhidrotic ectodermal dysplasia. *Neuropediatrics.* 1992;23(2):108-110.
4. Schweizer P, Kalhoff H, Horneff G, Wahn V, Diekmann L. [Polysaccharide specific humoral immunodeficiency in ectodermal dysplasia. Case report of a boy with two affected brothers]. *Klin Padiatr.* 1999;211(6):459-461.
5. Abinun M. Ectodermal dysplasia and immunodeficiency. *Arch Dis Child.* 1995;73(2):185.
6. Zonana J, Elder ME, Schneider LC, et al. A novel X-linked disorder of immune deficiency and hypohidrotic ectodermal dysplasia is allelic to incontinentia pigmenti and due to mutations in IKK-gamma (NEMO). *Am J Hum Genet.* 2000;67(6):1555-1562.
7. Courtois G, Smahi A, Israel A. NEMO/IKK gamma: linking NF-kappa B to human disease. *Trends Mol Med.* 2001;7(10):427-430.
8. Doffinger R, Smahi A, Bessia C, et al. X-linked anhidrotic ectodermal dysplasia with immunodeficiency is caused by impaired NF-kappaB signaling. *Nat Genet.* 2001;27(3):277-285.
9. Rothwarf DM, Zandi E, Natoli G, Karin M. IKK-gamma is an essential regulatory subunit of the IkappaB kinase complex. *Nature.* 1998;395(6699):297-300.
10. Yamaoka S, Courtois G, Bessia C, et al. Complementation cloning of NEMO, a component of the IkappaB kinase complex essential for NF-kappaB activation. *Cell.* 1998;93(7):1231-1240.
11. Smahi A, Courtois G, Vabres P, et al. Genomic rearrangement in NEMO impairs NF-kappaB activation and is a cause of incontinentia pigmenti. The International Incontinentia Pigmenti (IP) Consortium. *Nature.* 2000;405(6785):466-472.
12. Hanson EP, Monaco-Shawver L, Solt LA, et al. Hypomorphic nuclear factor-kappaB essential modulator mutation database and reconstitution system identifies phenotypic and immunologic diversity. *J Allergy Clin Immunol.* 2008;122(6):1169-1177.
13. Orange JS, Jain A, Ballas ZK, Schneider LC, Geha RS, Bonilla FA. The presentation and natural history of immunodeficiency caused by nuclear factor kappaB essential modulator mutation. *J Allergy Clin Immunol.* 2004;113(4):725-733.
14. Jain A, Ma CA, Liu S, Brown M, Cohen J, Strober W. Specific missense mutations in NEMO result in hyper-IgM syndrome with hypohydrotic ectodermal dysplasia. *Nat Immunol.* 2001;2(3):223-228.
15. Orange JS, Brodeur SR, Jain A, et al. Deficient natural killer cell cytotoxicity in patients with IKK-gamma/NEMO mutations. *J Clin Invest.* 2002;109(11):1501-1509.
16. Sebban H, Courtois G. NF-kappaB and inflammation in genetic disease. *Biochem Pharmacol.* 2006;72(9):1153-1160.
17. Nishikomori R, Akutagawa H, Maruyama K, et al. X-linked ectodermal dysplasia and immunodeficiency caused by reversion mosaicism of NEMO reveals a critical role for NEMO in human T-cell development and/or survival. *Blood.* 2004;103(12):4565-4572.
18. Mizukami T, Obara M, Nishikomori R, et al. Successful treatment with infliximab for inflammatory colitis in a patient with X-linked anhidrotic ectodermal dysplasia with immunodeficiency. *J Clin Immunol.* 2012;32(1):39-49.
19. Imamura M, Kawai T, Okada S, et al. Disseminated BCG infection mimicking metastatic nasopharyngeal carcinoma in an immunodeficient child with a novel hypomorphic NEMO mutation. *J Clin Immunol.* 2011;31(5):802-810.
20. Tono C, Takahashi Y, Terui K, et al. Correction of immunodeficiency associated with NEMO mutation by umbilical cord blood transplantation using a reduced-intensity conditioning regimen. *Bone Marrow Transplant.* 2007;39(12):801-804.
21. Saito M, Nishikomori R, Kambe N, et al. Disease-associated CIAS1 mutations induce monocyte death, revealing low-level mosaicism in mutation-negative cryopyrin-associated periodic syndrome patients. *Blood.* 2008;111(4):2132-2141.
22. Yang TP, Stout JT, Konecki DS, Patel PI, Alford RL, Caskey CT. Spontaneous reversion of novel Lesch-Nyhan mutation by HPRT gene rearrangement. *Somat Cell Mol Genet.* 1988;14(3):293-303.
23. Zhang LH, Jenssen D. Reversion of the hprt mutant clone SP5 by intrachromosomal recombination. *Carcinogenesis.* 1992;13(4):609-615.
24. Monnat RJ Jr, Chiaverotti TA, Hackmann AF, Maresh GA. Molecular structure and genetic stability of human hypoxanthine phosphoribosyltransferase (HPRT) gene duplications. *Genomics.* 1992;13(3):788-796.
25. Rautenstrauss B, Liehr T, Fuchs C, et al. Mosaicism for Charcot-Marie-Tooth disease type 1A: onset in childhood suggests somatic reversion in early developmental stages. *Int J Mol Med.* 1998;1(2):333-337.
26. Wada T, Candotti F. Somatic mosaicism in primary immune deficiencies. *Curr Opin Allergy Clin Immunol.* 2008;8(6):510-514.
27. Ariga T, Kondoh T, Yamaguchi K, et al. Spontaneous in vivo reversion of an inherited mutation in the Wiskott-Aldrich syndrome. *J Immunol.* 2001;166(8):5245-5249.
28. Stephan V, Wahn V, Le Deist F, et al. Atypical X-linked severe combined immunodeficiency due to possible spontaneous reversion of the genetic defect in T cells. *N Engl J Med.* 1996;335(21):1563-1567.
29. Rieux-Laucat F, Hivroz C, Lim A, et al. Inherited and somatic CD3zeta mutations in a patient with T-cell deficiency. *N Engl J Med.* 2006;354(18):1913-1921.
30. Wada T, Toma T, Okamoto H, et al. Oligoclonal expansion of T lymphocytes with multiple second-site mutations leads to Omenn syndrome in a patient with RAG1-deficient severe combined immunodeficiency. *Blood.* 2005;106(6):2099-2101.
31. Hirschhorn R. In vivo reversion to normal of inherited mutations in humans. *J Med Genet.* 2003;40(10):721-728.
32. Wada T, Schurman SH, Jagadeesh GJ, Garabedian EK, Nelson DL, Candotti F. Multiple patients with revertant mosaicism in a single Wiskott-Aldrich syndrome family. *Blood.* 2004;104(5):1270-1272.
33. Stewart DM, Candotti F, Nelson DL. The phenomenon of spontaneous genetic reversions in the Wiskott-Aldrich syndrome: a report of the workshop of the ESID Genetics Working Party at the XIIth Meeting of the European Society for Immunodeficiencies (ESID). Budapest, Hungary October 4-7, 2006. *J Clin Immunol.* 2007;27(6):634-639.
34. Davis BR, Yan Q, Bui JH, et al. Somatic mosaicism in the Wiskott-Aldrich syndrome: molecular and functional characterization of genotypic revertants. *Clin Immunol.* 2010;135(1):72-83.
35. Yamaoka S, Inoue H, Sakurai M, et al. Constitutive activation of NF-kappa B is essential for transformation of rat fibroblasts by the human T-cell leukemia virus type I Tax protein. *EMBO J.* 1996;15(4):873-887.
36. Speckmann C, Pannicke U, Wiech E, et al. Clinical and immunologic consequences of a somatic reversion in a patient with X-linked severe combined immunodeficiency. *Blood.* 2008;112(10):4090-4097.
37. Nenci A, Becker C, Wullaert A, et al. Epithelial NEMO links innate immunity to chronic intestinal inflammation. *Nature.* 2007;446(7135):557-561.
38. Fish JD, Duerst RE, Gelfand EW, Orange JS, Bunin N. Challenges in the use of allogeneic hematopoietic SCT for ectodermal dysplasia with immune deficiency. *Bone Marrow Transplant.* 2009;43(3):217-221.

Brief report

Identification of *TRIB1* R107L gain-of-function mutation in human acute megakaryocytic leukemia

Takashi Yokoyama,[1] Tsutomu Toki,[2] Yoshihiro Aoki,[2] Rika Kanezaki,[2] Myoung-ja Park,[3] Yohei Kanno,[1] Tomoko Takahara,[1] Yukari Yamazaki,[1] Etsuro Ito,[2] Yasuhide Hayashi,[3] and Takuro Nakamura[1]

[1]Division of Carcinogenesis, Cancer Institute, Japanese Foundation for Cancer Research, Tokyo, Japan; [2]Department of Pediatrics, Hirosaki University Graduate School of Medicine, Hirosaki, Japan; and [3]Department of Hematology/Oncology, Gunma Children's Medical Center, Gunma, Japan

Trib1 has been identified as a myeloid oncogene in a murine leukemia model. Here we identified a _TRIB1_ somatic mutation in a human case of Down syndrome–related acute megakaryocytic leukemia. The mutation was observed at well-conserved arginine 107 residue in the pseudokinase domain. This R107L mutation remained in leukocytes of the remission stage in which _GATA1_ mutation disappeared, suggesting the _TRIB1_ mutation is an earlier genetic event in leukemogenesis. The bone marrow transfer experiment showed that acute myeloid leukemia development was accelerated by transducing murine bone marrow cells with the R107L mutant in which enhancement of ERK phosphorylation and C/EBPα degradation by Trib1 expression was even greater than in those expressing wild-type. These results suggest that TRIB1 may be a novel important oncogene for Down syndrome–related acute megakaryocytic leukemia. (_Blood._ 2012; 119(11):2608-2611)

Introduction

The Down syndrome (DS) patients are predisposed to developing myeloid leukemia, and those patients frequently exhibit *GATA1* mutations.[1] However, it is proposed that the *GATA1* mutation is important for transient leukemia in DS but not sufficient for full-blown leukemia, suggesting that additional genetic alterations are needed.[1] Therefore, it is important to search the subsequent genetic changes for DS-related leukemia (ML-DS) to predict malignant transformation and prognosis of the patients.

Trib1 has been identified as a myeloid oncogene that cooperates with *Hoxa9* and *Meis1* in murine acute myeloid leukemia (AML).[2] As a member of the tribbles family of proteins, TRIB1 interacts with MEK1 and enhances ERK phosphorylation.[2,3] Moreover, TRIB1 promotes degradation of C/EBP family transcription factors, including C/EBPα, an important tumor suppressor for AML, and we observed that degradation of C/EBPα by Trib1 is mediated by its interaction with MEK1.[4] Thus, TRIB1 plays an important role in the development of AML by modulating both the RAS/MAPK pathway and C/EBPα function together with Trib2 that has also been identified as a myeloid-transforming gene.[5] Potential involvement of *TRIB1* in human leukemia has been reported in cases of AML with 8q34 amplification in which both *c-MYC* and *TRIB1* are included in the amplicon.[6] The enhancing effect of TRIB1 on the MAPK signaling suggests that TRIB1 alterations may be related to AML cases, which do not show any mutations in the pathway members, such as FLT3, c-Kit, or Ras. In this report, we identified a novel somatic mutation of *TRIB1* in a case of human acute megakaryocytic leukemia developed in DS (DS-AMKL). Retrovirus-mediated gene transfer followed by bone marrow transfer indicated that the mutation enhanced leukemogenic activity and MAPK phosphorylation by TRIB1.

Methods

Patients

TRIB1 mutations have been investigated in 12 cases of transient leukemia (TL), 5 of DS-AMKL, and 4 cell lines of DS-AML. Peripheral blood leukocytes of TL and bone marrow cells of DS-AMKL were used as sources for the molecular analysis. This study was approved by the Ethics Committee of Hirosaki University Graduate School of Medicine, and all clinical samples were obtained with informed consent from the parents of all patients, in accordance with the Declaration of Helsinki.

Patient 84 showed trisomy 21 and extensive leukocytosis at birth. Hematologic findings revealed the white blood cell count to be 148 × 10^9/L, including 87% myeloblasts, a hemoglobin level of 19.4 g/dL, and a platelet count of 259 × 10^9/L. Patent ductus arteriosus and atrial septal defect have been pointed out. Based on the hematologic data and the chromosomal abnormality, the patient was diagnosed as DS-related TL. The hematologic abnormality was then improved, but 8 months later 3% of 6.9 × 10^9/L white blood cells became myeloblasts (Figure 1A). A karyotype analysis of bone marrow cells revealed 48, XY,+8,+21 in 3 of 20 cells. In addition, *GATA1* mutation was detected at nt 113 from A to G, resulting in loss of the first methionine.[7] He was diagnosed as AMKL at this time, and his disease was in remission by subsequent chemotherapy.

PCR and sequencing

The entire coding region of human *TRIB1* cDNA of patients' samples was amplified using Taq polymerase (Promega) and specific primer pairs (the sequences of the primers are available on request). The genomic DNA samples of patient 84 were also analyzed. The sequence analysis of *GATA1* was performed as described previously.[7] After checking the PCR products by agarose gel electrophoresis, the products were purified and directly sequenced.

Submitted December 12, 2010; accepted January 6, 2012. Prepublished online as *Blood* First Edition paper, January 31, 2012; DOI 10.1182/blood-2010-12-324806.

The online version of this article contains a data supplement.

The publication costs of this article were defrayed in part by page charge payment. Therefore, and solely to indicate this fact, this article is hereby marked "advertisement" in accordance with 18 USC section 1734.

From bloodjournal.hematologylibrary.org at Hirosaki University on March 15, 2012. For personal use only.

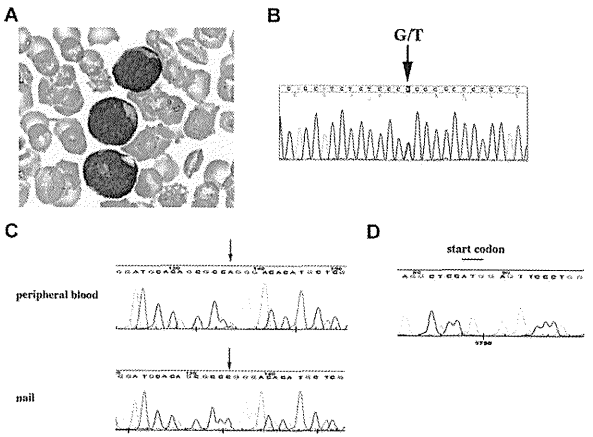

Figure 1. _TRIB1_ R107L mutation identified in DS-related leukemias. (A) Giemsa staining of the case 84 peripheral blood smear diagnosed as AMKL. The image was acquired using a BX40 microscope equipped with a 100×/1.30 NA oil objective (Olympus) and a C-4040 digital camera (Olympus). (B) Fluorescent dye sequencing chromatographs of *TRIB1* genotyping by direct sequencing of the case 84 using a cDNA sample as a template. The vertical arrow indicates mixed G and T signals at codon 107. (C) Fluorescent dye sequencing chromatographs of *TRIB1* of peripheral blood leukocytes (top) or nail (bottom) in the same case at the complete remission stage. The red arrows indicate that the mutation remains in leukocytes but not in nail. The reverse strand sequences are shown. (D) *GATA1* sequence. The start codon that was mutated in AMKL[7] is normal in the peripheral blood leukocytes at the remission stage.

Retroviral infection of murine bone marrow cells and bone marrow transfer

Bone marrow cells were prepared from 8-week-old female C57Bl/6J mice 5 days after injection of 150 mg/kg body weight of 5-fluorouracil (Kyowa Hakko Kogyo). Retroviral infection of bone marrow cells and bone marrow transfer experiments were performed as described.[2] Transduction efficiencies evaluated by flow cytometric techniques were comparable between wild-type (WT; 5.3%) and R107L (3.4%). Animals were housed, observed daily, and handled in accordance with the guidelines of the animal care committee at Japanese Foundation for Cancer Research. All the diseased mice were subjected to autopsy and analyzed morphologically, and the blood was examined by flow cytometric techniques. The mice were diagnosed as positive for AML according to the classification of the Bethesda proposal.[8] The survival rate of each group was evaluated using the Kaplan-Meier method, and differences between survival curves were compared using the log-rank test.

Immunoblotting

Immunoblotting was performed using cell lysates in RIPA buffer as described.[4] Anti-p44/42 ERK (Cell Signaling Technologies), anti–phospho-p44/42 ERK (Cell Signaling Technologies), anti-C/EBPα (Santa Cruz Biotechnology), anti-FLAG (Sigma-Aldrich), and anti-GAPDH (Hy Test Ltd) antibodies were used.

Results and discussion

The important role of TRIB1 on the MAPK signaling suggests that *TRIB1* alterations may occur in some AML cases, which do not show overlapping mutations in the pathway members, such as FLT3, KIT, or RAS. Therefore, we tried to search mutations of *TRIB1* in cases of ML-DS and TL in which such mutations are infrequent.[9] In a case of DS-AMKL (case 84), a nucleotide change from guanine to thymine has been identified at 902 that results in amino acid alteration from arginine 107 (R107) to leucine (Figure 1B). The sequence changes were confirmed by subcloning the PCR product into the TA-type plasmid vector (data not shown). The nucleotide change was not observed in the DNA sample derived from the nail of the same patient at all (Figure 1C), indicating that this change is a somatic mutation. Interestingly, the mutation was retained in the peripheral blood sample in the complete remission stage in which the GATA1 mutation completely disappeared (Figure 1C-D). These results indicate that the *TRIB1* mutation precedes the onset of TL and the *GATA1* mutation, and suggest that *TRIB1* mutation occurred at the hematopoietic stem cell level and that the clone retaining the *TRIB1* mutation survived after chemotherapy. In case 84, there was no mutation for *FLT3* exons 14, 15, and 20, *PTPN11* exons 3 and 13, *KRAS* exons 2, 3, and 5, and *KIT* exons 8, 11, and 17 by the high-resolution melt analysis (data not shown).

An additional mutation was found in a case of TL (case 109) at the nucleotides 805 and 806 from GC to AT, which results in amino acid conversion from alanine (A75) to isoleucine (supplemental Figure 1, available on the *Blood* Web site; see the Supplemental Materials link at the top of the online article). *TRIB1* expression in DS-related and DS-unrelated leukemias was examined by real-time quantitative RT-PCR (supplemental Figure 2).

R107 is located within a psuedokinase domain of TRIB1 that is considered as a functionally core domain of TRIB family proteins.[10] Sequence comparison among 3 TRIB family proteins as well as tribbles homologs in other organisms revealed that the R107 is well conserved in mammalian TRIB1 and TRIB2,[10] suggesting that this arginine residue is evolutionary conserved and may be related to an important function. On the other hand, A75 is located outside of the pseudokinase domain, not conserved between human and mouse, or other tribbles homologs. Moreover, the N-terminal domain containing A75 is dispensable for the leukemogenic activity of Trib1.[4] Therefore, we tried to investigate whether the R107L mutation could affect the leukemogenic activity of *TRIB1*.

R107L was introduced into the murine *Trib1* cDNA by site-directed mutagenesis. Both WT and R107L cDNAs were subcloned into the pMYs-IRES-GFP retroviral vector and were used for retrovirus-mediated gene transfer followed by bone marrow transfer according to the method previously described.[1] All the mice

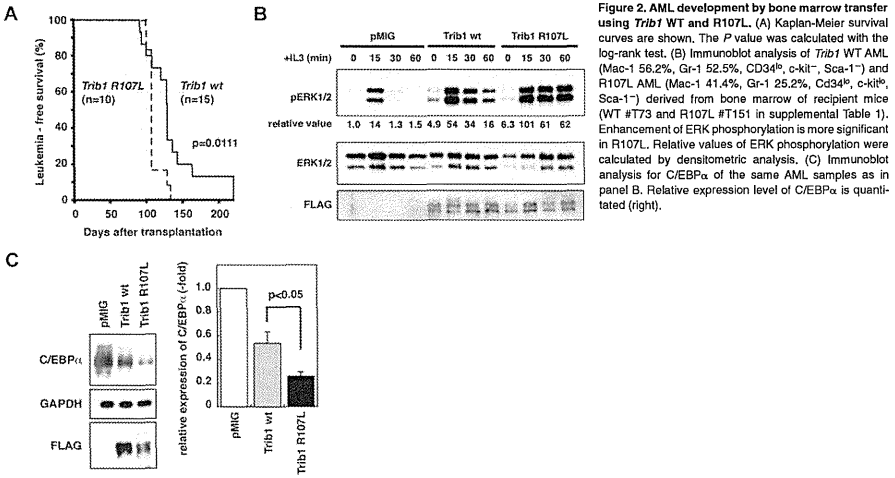

Figure 2. AML development by bone marrow transfer using *Trib1* WT and R107L. (A) Kaplan-Meier survival curves are shown. The *P* value was calculated with the log-rank test. (B) Immunoblot analysis of *Trib1* WT AML (Mac-1 56.2%, Gr-1 52.5%, CD34^{lo}, c-kil^{-}, Sca-1^{-}) and R107L AML (Mac-1 41.4%, Gr-1 25.2%, Cd34^{lo}, c-kit^{lo}, Sca-1^{-}) derived from bone marrow of recipient mice (WT #T73 and R107L #T151 in supplemental Table 1). Enhancement of ERK phosphorylation is more significant in R107L. Relative values of ERK phosphorylation were calculated by densitometric analysis. (C) Immunoblot analysis for C/EBPα of the same AML samples as in panel B. Relative expression level of C/EBPα is quantitated (right).

transplanted with bone marrow cells expressing WT (n = 15) or R107L (n = 12) developed AML (Figure 2A). The mean survival time was shorter in the recipients with R107L-expressing bone marrow cells (110 days) than those with WT (136 days; Figure 2A). The difference was significant ($P = .0111$, log-rank test). The result indicates that the R107L mutation enhances the leukemogenic activity of TRIB1. These results also suggest that *TRIB1* mutation might cooperate with *GATA1* mutation in the genesis of DS-AMKL, and that trisomy 21, *TRIB1*, and *GATA1* mutations occurred consecutively, which contributed to the multistep leukemogenic process.

We have shown that TRIB1 interacts with MEK1 and enhances phosphorylation of ERK.[2] The R107L mutant enhanced ERK phosphorylation more extensively than WT (Figure 2B) in AML cells derived from bone marrow of recipient mice, and more significant degradation of C/EBPα was induced by the R107L mutant (Figure 2C). These findings might be correlated to the enhanced leukemogenic activity of the mutant. Both R107L and WT proteins could interact with MEK1, having the binding motif in their C-termini. The residue 107 is located at subdomain II of the pseudokinase domain.[11] The mutation may affect conformation of the domain and may promote the MEK1 function on ERK, although additional studies are required to address the possibility. A recent study demonstrates that Trib1 and Trib2 failed to show ERK phosphorylation in 32D cells.[12] The different response to Trib1 between primary leukemic cells and the cell line might depend on the cellular context and/or combination of additional mutations. The AML phenotypes were somewhat varied in each case and Mac-1–positive/Gr-1–negative AMLs were more remarkable in WT than in R107L, although the difference was not statistically significant (supplemental Figures 3-4; supplemental Table 1). The current study underscores the role of TRIB1 in human leukemogenesis and the significance of the R107L mutation in its function. Further sequence analysis of tribbles family genes in a larger cohort will emphasize the importance of R107L and/or additional mutations of *TRIB1* in leukemic patients.

Acknowledgments

This work was supported by KAKENHI (Grant-in-Aid for Scientific Research) on Priority Areas Integrative Research Toward the Conquest of Cancer (E.I. and T.N.) and the Ministry of Education, Culture, Sports, Science and Technology of Japan (Young Scientists, T.Y.).

Authorship

Contribution: T.Y., E.I., Y.H., and T.N. designed and performed the research and wrote the manuscript; T. Toki, Y.A., R.K., and M.-j.P. performed the research; and Y.K., T. Takahara, and Y.Y. contributed to the bone marrow transplantation analysis.

Conflict-of-interest disclosure: The authors declare no competing financial interests.

Correspondence: Takuro Nakamura, Division of Carcinogenesis, Cancer Institute, Japanese Foundation for Cancer Research, 3-8-31 Ariake, Koto-ku, Tokyo 135-8550, Japan; e-mail: takuro-ind@umin.net.

References

1. Shimizu R, Engel JD, Yamamoto M. GATA1-related leukaemias. *Nat Rev Cancer.* 2008;8(4):279-287.
2. Jin G, Yamazaki Y, Takuwa M, et al. Trib1 and Evi1 cooperate with Hoxa and Meis1 in myeloid leukemogenesis. *Blood.* 2007;109(9):3998-4005.
3. Kiss-Toth E, Bagstaff SM, Sung HY, et al. Human Tribbles, a protein family controlling mitogen-activated protein kinase cascades. *J Biol Chem.* 2004;279(41):42703-42708.
4. Yokoyama T, Kanno Y, Yamazaki Y, et al. Trib1 links the MEK/ERK pathway in myeloid leukemogenesis. *Blood.* 2010;116(15):2768-2775.
5. Keeshan K, He Y, Wouters BJ, et al. Tribbles homolog 2 inactivates C/EBPalpha and causes acute myelogenous leukemia. *Cancer Cell.* 2006;10(5):401-411.
6. Storlazzi CT, Fioretos T, Surace C, et al. MYC-containing double minutes in hematologic malignancies: evidence in favor of the episome model and exclusion of MYC as the target gene. *Hum Mol Genet.* 2006;15(6):933-942.
7. Kanezaki R, Toki T, Terui K, et al. Down syndrome and GATA1 mutations in transient abnormal myeloproliferative disorder: mutation classes correlate with progression to myeloid leukemia. *Blood.* 2010;116(22):4631-4638.
8. Kogan SC, Ward JM, Anver MR, et al. Bethesda proposal for classification of nonlymphoid hematopoietic neoplasms in mice. *Blood.* 2002;100(1):238-245.
9. Toki T, Kanezaki R, Adachi S, et al. The key role of stem cell factor/KIT signaling in the proliferation of blast cells from Down syndrome-related leukemia. *Leukemia.* 2009;23(1):95-103.
10. Hegedus Z, Czibula A, Kiss-Toth E. Tribbles: a family of kinase-like proteins with potent signaling regulatory function. *Cell Signal.* 2007;19(2):238-250.
11. Yokoyama T, Nakamura T. Tribbles in disease: signaling pathways important for cellular function and neoplastic transformation. *Cancer Sci.* 2011;102(6):1115-1122.
12. Dedhia PH, Keeshan K, Uljon S, et al. Differential ability of Tribbles family members to promote degradation of C/EBPalpha and induce acute myelogenous leukemia. *Blood.* 2010;116(8):1321-1328.

A Novel Mutation of Ribosomal Protein S10 Gene in a Japanese Patient With Diamond-Blackfan Anemia

Makoto Yazaki, MD, Michi Kamei, MD,† Yasuhiko Ito, MD,† Yuki Konno, MD,‡ RuNan Wang, MD,‡ Tsutomu Toki, MD,‡ and Etsuro Ito, MD‡*

Summary: Diamond-Blackfan anemia (DBA) is an inherited bone marrow disease. The condition is characterized by anemia that usually presents during infancy or early childhood and congenital malformation. Several reports show that DBA is associated with mutations in the ribosomal protein (RP) genes, *RPS19*, *RPS24*, *RPS17*, *RPL35A*, *RPL5*, *RPL11*, and *RPS7*. Recently, 5 and 12 patients with mutations in *RPS10* and *RPS26*, respectively, were identified in a cohort of 117 DBA probands. Therefore, we screened the DBA patients who were negative for mutations in these DBA genes for mutations in *RPS10* and *RPS26*. The present case report describes the identification of the first Japanese DBA patient with a novel mutation in *RPS10*.

Key Words: Diamond-Blackfan anemia, ribosomal protein genes, mutation in *RPS10*

(*J Pediatr Hematol Oncol* 2012;34:293–295)

Diamond-Blackfan anemia (DBA) is an inherited bone marrow disease. The condition is characterized by anemia that usually presents during infancy or early childhood, congenital malformation, and an increased incidence of cancer.[1–3] In 1999, it was reported that DBA is associated with mutations in the ribosomal protein (RP) gene, *RPS19*.[4] This mutation was identified in 25% of DBA probands and prompted the search for other RP gene mutations. Subsequently, DBA patients with mutations in *RPS24*, *RPS17*, *RPL35A*, *RPL5*, *RPL11*, and *RPS7* were reported, suggesting that DBA is a disorder of ribosomal biogenesis and/or function.[5–7] Recently, Doherty et al[8] reported 3 distinct mutations of the *RPS10* in 5 patients from a cohort of 117 DBA probands. Therefore, we screened the Japanese DBA patients who were negative for mutations in these RP genes for mutations in *RPS10* and *RPS26*. Here, we report the first Japanese DBA patient with a novel mutation in *RPS10*.

Received for publication September 14, 2011; accepted January 8, 2012.
From the *Department of Pediatrics, Nagoya City East Medical Center Moriyama Hospital; †Department of Pediatrics and Neonatology, Nagoya City University Graduate School of Medical Science, Nagoya; and ‡Department of Pediatrics, Hirosaki University Graduate School of Medicine, Hirosaki, Japan.
This study was supported in part by a grant from Health and Labor Sciences Research Grants (Research on intractable diseases) from the Ministry of Health, Labour, and Welfare of Japan.
The authors declare no conflict of interest.
Reprints: Makoto Yazaki, MD, Department of Pediatrics, Nagoya City East Medical Center Moriyama Hospital, 18-22 2-chome, Moriyama, Moriyama-ku, Nagoya 463-8567, Japan (e-mail: yazakim@mild.ocn.ne.jp).

CASE REPORT

A 6-year-old boy was referred to our hospital with anemia with no other significant cytopenia. He was an only child with no family history of anemia. He has no congenital malformations described in "classical DBA," apart from bilateral lymphangioma of the foot. His white blood cell count was 4.3×10^9/L, the erythrocyte count was 2540×10^9/L, the hematocrit was 24.6%, hemoglobin concentration was 8.3 g/dL, the mean corpuscular volume was 96.9 fl, the mean corpuscular hemoglobin was 32.7 pg, the platelet count was 278×10^9/L, and the reticulocyte count was 1.5%. The fetal hemoglobin was 1.4%. The serum iron was 93 μg/dL, the serum unsaturated iron-binding capacity was 184 μg/dL, and the serum ferritin was 9 ng/mL. The serum vitamin B12 was 850 pg/mL and the serum folic acid was 6.8 ng/mL. The serum aspartate aminotransferase was 17 U/mL, the alanine aminotransferase was 10 U/mL, and the lactate dehydrogenase was 201 U/mL. The erythropoietin level was 1170 mU/L. The serum total bilirubin was 0.5 mg/dL. The direct and indirect Coombs' tests were negative. The anti-B19 parvovirus immunoglobulin M and immunoglobulin G antibodies were negative. Bone marrow aspiration showed that the cellularity was slightly hypoplastic (78500/μL), with a paucity of erythroid cells (16.8%; macrocytic-basophilic erythroblasts, 0.4%, noromocytic-basophilic erythrobalasts, 1.2%, noromocytic-polychromic erythroblasts, 10.4%, normocytic-orthochromic erythroblasts, 4.8%), but the morphology was normal. It showed that myeloid cells (34.4%) have no abnormalities associated with myelodysplastic syndromes. Lymphoid cells (38%) and megakaryocytes were normal. Cytogenetic analysis showed no chromosomal abnormality. On the basis of these findings, DBA was diagnosed in this patient.[1] The patient responded to oral steroids but not to cyclosporine. A small dose of prednisolone (0.18 to 0.23 mg/kg/d) were given to maintain an erythrocyte count of 2500×10^9/L, a hemoglobin concentration of 8.0 g/dL, and his daily activities. The most distressing complication has been obesity. He has never received blood transfusion.

At 22 years of age, analysis of RP genes was performed. Informed consent was obtained according to the guidelines set out by Hirosaki University Graduate School of Medicine. Initially, the patient was screened for mutations in the 8 genes known to be associated with DBA, *RPS19*, *RPS24*, *RPS17*, *RPL5*, *RPL11*, *RPL35A*, *RPS10*, and *RPS26*, using high-resolution amplicon melting analysis. He was also screened for *RPS14* mutations, which are a causative gene for 5q-syndrome. The results showed a separated signal derived from the heteroduplex polymerase chain reaction product from the third exon of *RPS10*. Direct sequencing analysis of the polymerase chain reaction product and the cloned amplicon identified a heterozygous mutation (283_306delinsTGCC) (Fig. 1). This mutation resulted in a frameshift at codon 95 and a "stop" at codon 100 (Fig. 2).

DISCUSSION

Nine RP genes, *RPS19*, *RPS24*, *RPS17*, *RPL5*, *RPL11*, *RPL35A*, *RPS14*, *RPS10*, and *RPS26*, were screened in 64 Japanese probands with DBA. Screening identified 8, 6, and 3 patients with mutations in *RPS19*, *RPL5*, and *RPL11*, respectively, and a single patient each with a mutation in *RPS17*, *RPS10*, and *RPS26*[9] and (unpublished data). In total, 20 (31.3%) of the Japanese DBA patients had mutations in RP genes. This is a slightly lower frequency than that reported in Western countries, although the data from both populations are based on relatively low numbers of patients, and data showing significant differences between populations are lacking.

The RPSP10 gene is located on chromosome 6 and contains 6 exons, with the start codon in exon 2. *RPS10* encodes a protein of 165 amino acids, which is a component of the 40S ribosomal subunit. To our knowledge, this is the first report of a Japanese DBA patient with a mutation in *RPS10*. The mutation (283_306delinsTGCC) results in a frameshift at codon 95 and the premature termination of codon 100. This novel mutation has not been reported in the literature. Doherty et al[8] identified 3 heterozygous sequence changes in *RPS10* in 5/117 probands, with no evidence of mutations in any of the known DBA genes. One sequence change was a missense mutation 3G > A (Met1 to Ile), which eliminates the start codon. The next downstream start codon is located at nucleotide position 61 to 63 and is predicted to start translation of a truncated protein. Another mutation was c.260.261insC, which results in a frameshift at codon 87 and a "stop" at codon 97. Three other probands contained a common nonsense mutation, c.337C > T, causing an Arg113 "stop." In our case, the mutation seems to be the result of both a deletion and an insertion. These mutations are very rare in DBA. To understand the mechanism of mutagenesis, we examined *RPS10* psuedogenes (*PRS10P1* to *RPS10P3*1) to see if this mutation arose from interlocus gene conversion. However, we could find no evidence that the mutation arose due to gene conversion. The authors estimated that *RPS10* mutations were present in about 2.6% of the DBA population. Although more information is needed to estimate the incidence of *RPS10* mutations in Japanese DBA patients, the frequency of *RPS10* mutations in the Japanese population was similar to that in Western countries. All the *RPS10* mutations observed in patients with DBA, including our case, are nonsense or frameshift mutations. Nonsense and frameshift mutations are likely to be pathogenic in the majority of cases; however, determining the pathogenicity of a particular missense mutation may be difficult.

The RPS19 protein plays an important role in 18S rRNA maturation in both yeast and human cells.[10–13] Other

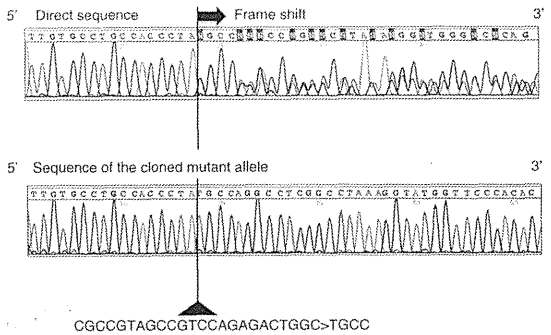

FIGURE 1. Sequence changes and frameshift in the *RPS10*. Direct sequencing showed a separated signal derived from the heteroduplex polymerase chain reaction product from the third exon of *RPS10*. Sequencing of the cloned mutant allele identified a heterozygous mutation (c.283_306delinsTGCC) and frameshift.

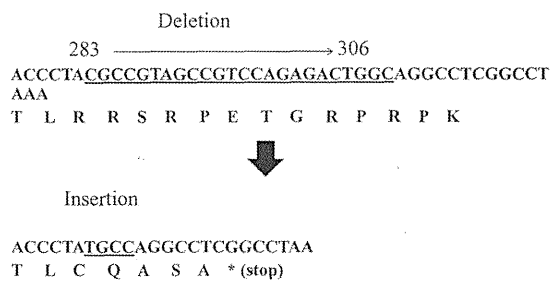

FIGURE 2. Deletion and insertion of this patient in *RSP10*. The c.283_306delinsTGCC mutation resulted in a frameshift at codon 95 and a "stop" at codon 100.

studies demonstrate alterations of pre-RNA processing and small or large ribosomal subunit synthesis in human cells with *RPS24*, *RPS7*, *RPL35A*, *RPL5*, and *RPL11* deficiency.[14–16] Increased apoptosis has been demonstrated in hematopoietic cell lines and bone marrow cells deficient in RPS19 and RPL35A.[14,17,18] Imbalances in p53 family proteins have been suggested as a mechanism of abnormal embryogenesis and anemia in zebrafish upon perturbation of RPS19 expression.[19] Also, the DBA phenotype in mice was ameliorated by knockdown of p53.[20] We hope to use hematopoietic progenitor cells to investigate why mutations in *RPS10* affect erythropoiesis in DBA patients.

Patients with "classical DBA" fulfill all the major diagnostic criteria, including anemia presenting before the first birthday.[1] However, a definitive diagnosis of DBA is often difficult because of incomplete phenotypes and a wide variation in clinical expression. This particular patient presented with macrocytic anemia at 6 years of age, with no family history and none of the congenital anomalies described for "classical DBA." The identification of pathogenic mutations in *RPS10* provides a definitive diagnosis of DBA in this patient. Although the use of molecular diagnostic techniques is essential to establish a definitive diagnosis and research the cause of DBA, such a diagnosis in only obtained for 30% to 40% of patients. Therefore, it is important to identify all genes that cause DBA if we are to improve the efficiency of molecular diagnostic techniques and understand the pathogenesis of DBA.

REFERENCES

1. Vlachos A, Ball S, Dahl N, et al. Diagnosing and treating Diamond Blackfan anaemia: results of an international clinical consensus conference. *Br J Haematol*. 2008;142:859–876.
2. Gazda HT, Sieff CA. Recent insights into the pathogenesis of Diamond-Blackfan anemia. *Br J Haematol*. 2006;135:149–157.
3. Flygare J, Karlsson S. Diamond-Blackfan anemia: erythropoiesis lost in translation. *Blood*. 2007;109:3152–3160.
4. Draptchinskaia N, Gustavsson P, Andersson B, et al. The gene encoding ribosomal protein S19 is mutated in Diamond-Blackfan anemia. *Nat Genet*. 1999;21:169–175.
5. Gazda HT, Grabowska A, Merida-Long LB, et al. Ribosomal protein S24 gene is mutated in Diamond-Blackfan anemia. *Am J Hum Genet*. 2006;79:1110–1118.
6. Cmejla R, Cmejlova J, Handrkowa H, et al. Ribosomal protein S17 gene (RPS17) is mutated in Diamond-Blackfan anemia. *Hum Mutat*. 2007;28:1178–1182.
7. Ito E, Konno Y, Toki T, Terui K. Molecular pathogenesis in Diamond-Blackfan anemia. *Int J Hematol*. 2010;92:413–418.
8. Doherty L, Sheen MR, Vlachos A, et al. Ribosomal protein genes RPS10 and RPS26 are commonly mutated in Diamond-Blackfan anemia. *Am J Hum Genet*. 2010;86:222–228.
9. Konno Y, Toki T, Tandai S, et al. Mutations in the ribosomal protein genes in Japanese patients with Diamond-Blackfan anemia. *Haematologica*. 2010;95:1293–1299.
10. Léger-Silvestre I, Caffrey JM, Dawaliby R, et al. Specific role for yeast homologs of the Diamond Blackfan anemia-associated RPS19 protein in ribosome synthesis. *J Biol Chem*. 2005;280:38177–38185.
11. Choesmel V, Bacqueville D, Rouquette J, et al. Impaired ribosome biogenesis in Diamond-Blackfan anemia. *Blood*. 2007;109:1275–1283.
12. Flygare J, Aspesi A, Bailey JC, et al. Human RPS19, the gene mutation in Diamond-Blackfan anemia, encodes a ribosomal protein required for the maturation of 40S ribosomal subunits. *Blood*. 2007;109:980–986.
13. Idol RA, Robledo S, Du HY, et al. Cells depleted for RPS19, protein associated in Diamond-Blackfan anemia, show defects in 18S ribosomal RNA synthesis and small ribosomal subunit production. *Blood Cell Mol Dis*. 2007;39:35–43.
14. Farrar JE, Nater M, Caywood E, et al. Abnormalities of the large ribosomal subunit protein, Rpl35a, in Diamond-Blackfan anemia. *Blood*. 2008;112:1582–1592.
15. Gazda HT, Sheen MR, Vlachos A, et al. Ribosomal Protein L5 and L11 mutations are associated with cleft palate and abnormal thumbs in Diamond-Blackfan anemia patients. *Am J Hum Genet*. 2008;83:769–780.
16. Choesmel V, Fribourg S, Aguissa-Touré AH, et al. Mutation of ribosomal protein RPS24 in Diamond-Blackfan anemia results in ribosome biogenesis disorder. *Hum Mol Genet*. 2008;17:1253–1263.
17. Perdahl EB, Naprstek BJ, Wallace WC, et al. Erythroid failure in Diamond-Blackfan anemia is characterized by apoptosis. *Blood*. 1994;83:645–650.
18. Miyake K, Utsugisawa T, Flygare J, et al. Ribosomal protein S19 deficiency leads to reduced proliferation and increased apoptosis but does not affect terminal erythroid differentiation in a cell line model of Diamond-Blackfan anemia patients. *Stem Cells*. 2008;26:323–329.
19. Danilova N, Sakamoto KM, Lin S. Ribosomal protein S19 deficiency in zebrafish leads to developmental abnormalities and defective erythropoiesis through activation of p53 protein family. *Blood*. 2008;112:5228–5237.
20. McGowan KA, Li JZ, Park CY, et al. Ribosomal mutations cause p53-mediated dark skin and pleiotropic effect. *Nat Genet*. 2008;40:963–970.

5．骨髄不全症候群における テロメア制御異常

山口　博樹[1]・檀　和夫[2]
Yamaguchi Hiroki　Dan Kazuo

日本医科大学 血液内科 [1]講師 [2]主任教授

Summary　Dyskeratosis congenita (DKC) は，網状色素沈着，爪の萎縮，舌などの粘膜白斑症を伴う遺伝性骨髄不全症である。テロメラーゼ複合体を構成する遺伝子群，Shelterin 複合体を構成する *TINF2*，テロメラーゼ複合体を核内の Cajalbody に移行させる *TCAB1* が DKC の責任遺伝子として同定された。DKC は，これらの遺伝子変異が原因のテロメア制御不全に，世代促進や加齢が加わることでテロメアが短縮化し，その結果造血幹細胞などの増殖能に障害が生じて発症すると考えられている。しかし，依然として確立した治療法はなく，さらなる病態の解析による新たな治療法が期待される。

はじめに

テロメアは染色体の末端部位に存在する繰り返し配列を持つ DNA（ヒトでは 5'-TTAGGG-3'）と，そこに局在するテロメラーゼ複合体や Shelterin 複合体などの種々の蛋白質から構成されている[1]。テロメアはその構造から，他の要因で受けた DNA 切断末端と区別され，DNA の分解や修復から染色体を保護し，物理的および遺伝的な安定性を保つ働きをしている[1]。

ヒトなどの動物組織から取り出した培養細胞は，複数回の分裂を繰り返すとテロメア長が短縮化し細胞分裂が停止する，細胞老化という現象が認められる[2,3]。これは細胞分裂の際に DNA 複製が行われるが，リーディング鎖は完全にコピーされるのに対して，ラギング鎖は最終の岡崎フラグメントから約 200 bp 離れたところに複製のためのプライマーが合成されるため，3' 末端の一部はコピーが不完全となるためである[1,4,5]。また，仮に偶然 3' 末端にプライマーが合成されても，複製後プライマーは DNA に変換されないため，テロメアの短縮化は避けられない[1,4,5]。しかし，造血幹細胞や生殖細胞などでは，テロメラーゼによるテロメア長の伸長補正が行われるため，常に細胞分裂が可能である[1]。

近年，このテロメア長の伸長補正の障害が，Dyskeratosis congenita（DKC），一部の再生不良性貧血や骨髄異形性症候群，特発性肺線維症の原因と同定され，さらには猫鳴き症候群，急性骨髄性白血病，肝硬変などの病態への関与も示唆されている[6~9]。本稿では，DKC などの骨髄不全症候群とテロメア制御異常に関して概説する。

DKC (Dyskeratosis congenita)

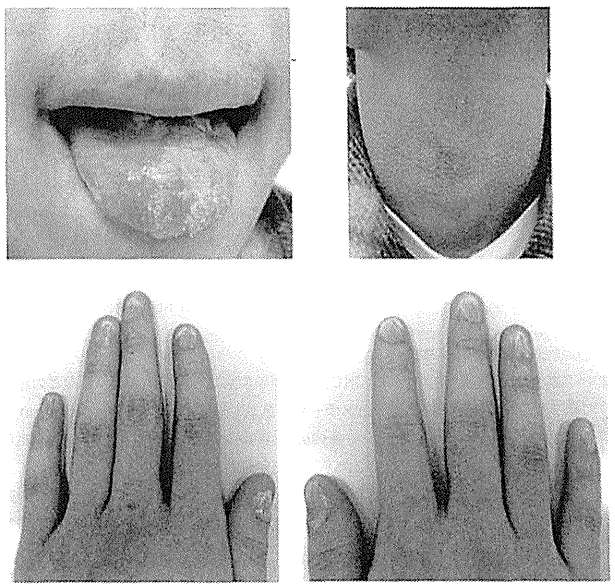

図1　DKC の特徴的身体所見
DKC の特徴的身体所見を示す。左上段：舌の粘膜白斑症，右上段：網状色素沈着，下段：爪の萎縮。（筆者提供）

1．DKC における テロメア関連遺伝子異常

DKC は網状色素沈着，爪の萎縮，舌などの粘膜白斑症を伴う骨髄不全症（Bone marrow failure：BMF）で，10 歳前後までに約 80%以上の症例にこれらの特徴的身体所見が付随し BMF を発症する（図1）[7]。そして上記以外にも，精神発育遅滞，肺疾患，低身長，歯の異常，食道狭窄，頭髪の喪失，白髪などの多彩な合併症が 15 ～ 25%の症例に認められ，また 8%の症例に皮膚，上咽頭，消化管の扁平上皮癌や腺癌などの悪性腫瘍や，骨髄異形成症候群（MDS），Hodgkin 病，急性骨髄性白血病などの造血器腫瘍の発生が認められる[7]。

遺伝型式は X 連鎖劣性遺伝が約 35%，常染色体優性遺伝が約 15%，常染色体劣性遺伝が数%

BMF (Bone marrow failure；骨髄不全症)　MDS (骨髄異形成症候群)

表1　テロメア関連遺伝子変異と疾患

遺伝子（蛋白）	染色体存在部位	DKC における変異頻度	変異の type	疾患
Telomerase				
TERC	3q21-28	5～10%	Heterozygous	AD-DKC, AA, ET, MDS PNH, PF
TERT (TERT)	5p15.33	5%	Heterozygous	AD-DKC, AA, HHS, PF
			Biallelic	AR-DKC, HHS
DKC1 (Dyskerin)	Xq28	30%	Heterozygous	X-linked DKC, HHS
NHP2 (NHP2)	5q35.3	< 1%	Biallelic	AR-DKC
NOP10 (NOP10)	15q14-q15	< 1%	Heterozygous	AR-DKC
TCAB1	17p13.1	< 1%	Biallelic	AR-DKC
Shelterin				
TINF2 (TINF2)	14q11.2	10～15%	Heterozygous	AD-DKC, AA, HHS, RS

AD-DKC：常染色体優性遺伝型 DKC，AA：再生不良性貧血，ET：本態性血小板血症，MDS：骨髄異形成症候群，PNH：発作性夜間ヘモグロビン尿症，PF：肺線維症，HHS：Hoyeraal-Hreidarsson syndrome，X-kinked DKC：X連鎖劣性遺伝型 DKC，AR-DKC：常染色体劣性遺伝型 DKC，RS：Revesz Syndrome

DKC は表に記載した遺伝子変異によりテロメアが短縮化し，その結果造血幹細胞などの増殖能に障害が生じ，骨髄不全症や網状色素沈着，爪の萎縮，舌などの粘膜白斑症の症候が形成されると考えられている。（文献7より改変）

に認められるが，残りの約40%近くが型式不明である[7]。近年，テロメラーゼ複合体を構成する遺伝子群である，*DKC1*，*telomerase RNA component*（***TERC***），*telomerase reverse transcriptase*（***TERT***），*NOP10*，*NHP2*，Shelterin 複合体を構成する *TRF-interacting nuclear protein*（***TINF2***），テロメラーゼ複合体を核内の Cajalbody に移行させる *TCAB1* が DKC の責任遺伝子として同定された（**表1**）[6～10]。DKC はこれらの遺伝子の変異によりテロメアが短縮化し，その結果造血幹細胞などの増殖能に障害が生じ，前述の症候が形成されると考えられている[7]。

また，DKC の発症年齢，随伴症状，造血障害の有無とテロメアの短縮化の程度には相関がみられ，後述の DKC の重症型と考えられている Hoyeraal-Hreidarsson syndrome（HHS）は，DKC と比較してテロメアの短縮が著しいと報告されている[11]。

HHS は男児の幼時期に骨髄不全症を発症する遺伝性疾患である。骨髄不全症以外には小頭症，小脳低形成，成長発達遅延，顔貌異常，B細胞とNK細胞数の低下，細胞性免疫不全を合併し，大多数の症例は10歳前後で死亡する[12]。遺伝型式の大多数はX連鎖劣性遺伝の男児とされてきたが，女児の HHS も報告されるようになった[12]。最近の報告では HHS の 1/3 の症例は女児で，その遺伝型式は常染色体劣性遺伝とされている[13]。HHS は独立した疾患として考えられていたが，その後 HHS に *DKC1*，*TERT* などのテロメア制御遺伝子変異が発見され，DKC の重症型と考えられるようになった[12, 13]。

2．X連鎖劣性遺伝型の DKC

DKC1 遺伝子（***DKC1***）は，染色体 Xq28 上にコードされ，X連鎖劣性遺伝型の DKC の原因遺伝子である。*DKC1* によって翻訳される Dyskerin は核内蛋白の small nucleolar RNAs（snoRNA）

TERC（*telomerase RNA component*）　*TERT*（*telomerase reverse transcriptase*）　*TINF2*（*TRF-interacting nuclear protein*）
HHS（Hoyeraal-Hreidarsson syndrome）　*DKC1*（*DKC1* 遺伝子）　snoRNA（small nucleolar RNAs）

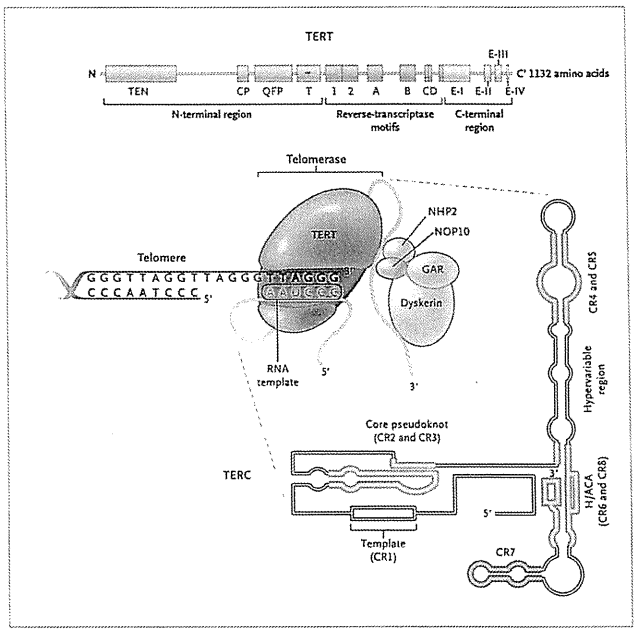

図2　テロメラーゼ複合体

TERC は自身で2次構造を形成し，5'側の pseudoknot ドメインと CR4-CR5 ドメインは TERT と結合し，テロメラーゼ活性に関与している。一方，3'側の boxH/ACA ドメインは Dyskerin などの snoRNA 蛋白と結合し，CR7 ドメインは small Cajalbody RNAs 蛋白（scaRNAs）と CAB box を介して結合することで，テロメラーゼ複合体の processing や stability に関与している。（文献9より改変）

の一つで，boxH/ACA ドメインを持ち，他の snoRNA である NOP10，NHP2，GAR1 と複合体を形成し，ribosomal RNA（rRNA）の processing や pre rRNA の転写産物の翻訳後修飾（pseudouridylation）に関与していると考えられている[14]。また，Dyskerin を含む snoRNA 複合体は *TERC* の boxH/ACA ドメインと結合し，テロメラーゼ複合体の processing と安定化の役割を果たしている（**図2**）[14]。

X連鎖型の DKC はこの *DKC1* の変異によって引き起こされると考えられているが，その変異の大多数は point mutation で，large deletion やスプライス変異は稀である。これは *DKC1* の knockout マウスは胎性致死を起こすことから，Dyskerin は細胞の生存に必須の蛋白であるためではないかと予想される[15]。*DKC1* の変異は

rRNA（ribosomal RNA）

exon 3，4，10，11，12に集中しており，中でもexon 11のPUA pseudouridin合成酵素モチーフ上には多くの変異が認められる。特に，*DKC1*変異の約30%に認められるA353Vはhot spotと考えられており，*TERC*とsnoRNAのaccumulation，テロメラーゼ活性，rRNA processingやpseudouridylationに障害を与え，DKCの病態への関与が示されている[16]。また，TruB pseudouridin合成酵素モチーフの存在する領域の変異であるS121GやR158Wが，DKCの重症型と考えられているHHSの表現型を示すことは興味深い点である[12]。しかし，DKCとHH両者に認められる変異も存在し，変異部位とDKCの重症度，HHSとの関連には不明な点が多い[11,12]。さらに，*DKC1*のpromoter領域には3つのGC-rich *cis*-elementsが存在し，Sp1とSp3により*DKC1*の発現が調節されている。そのSp1 binding siteの変異である－141C/Gが*DKC1*の発現量を低下させDKCを発症させることが報告されており，DKCはDyskerinの変異による質的な異常だけでなく，量的な異常でも発症することが示唆されている[17]。

DKCのモデルとしては，*DKC1*のexon 12-15の欠損またはexon 15のみ欠損するDyskerin hypomorphic変異マウスでの解析が行われている[18]。この*DKC1*の発現を著しく低下させたモデルマウスでは，最初の第2世代目までにDKCの表現型が再現される。興味深いことに，DKCの表現型が再現される第2世代目では，rRNAのprocessingや*mTERC*の発現とテロメラーゼ活性の低下は認められるが，テロメア長の短縮は認められず，第4世代目になってようやくテロメア長の短縮化が認められる[18]。このことは，DKCの病態の形成にリボゾームの機能障害が関与していることを示している。

3．常染色体優性遺伝型のDKC

1）*TERC*と*TERT*遺伝子変異

常染色体優性遺伝型のDKCの原因遺伝子としては，テロメラーゼ複合体の*TERC*と*TERT*が同定されている。*TERC*は染色体3q21-28上にコードされ，蛋白に翻訳されない451 bpのRNAとしてテロメア伸展における鋳型の役割をしている[1,19]。*TERC*は自身で2次構造を形成し，5'側のpseudoknotドメインとCR4-CR5ドメインは，TERTと結合してテロメラーゼ活性に関与している[1,19]。一方，3'側のboxH/ACAドメインはDyskerinなどのsnoRNA蛋白と結合し，CR7ドメインはsmall Cajalbody RNAs蛋白（scaRNAs）とCAB boxを介して結合することで，テロメラーゼ複合体のprocessingやstabilityに関与している（図2）[1,19]。scaRNAs蛋白は核内のCajalbodyに存在し，snoRNAと同様にrRNAに対してのpseudouridylationやmethylationなどを修飾する機能があると考えられている[20]。一方，テロメラーゼ複合体において逆転写酵素の役割をもつ*TERT*は，染色体5p15にコードされ*TERC* bindingの機能があるN-terminus，7つのconserved motifsがあり逆転写活性をもつreverse transcriptase（RT）と，telomerase multimerizationの機能があるC-terminuの3つのregionで構成されている（図2）[1,19]。

常染色体優性遺伝型のDKCの特徴は，X連鎖劣性遺伝型のDKCと比較して症状や検査所見の異常が軽度である症例が多いということである[6~8]。これは，後述の不全型DKCでは*DKC1*変異は認められず，その大多数において*TERC*や*TERT*の変異が認められることからも推測される[6~9]。*In vitro*の機能解析では，*TERC*の鋳型となる配列の変異はdominant negative効果でテロメラーゼ活性を減弱させるが，その他の変異はhaploinsufficiency効果を示し，テロメラーゼ活性の減弱の程度は弱く，このことが常染色体優性遺伝型のDKCの症状や検査所見の異常が軽度である一つの理由として考えられている[21~23]。また，モデルマウスでも同様の結果が得られており，前述の*DKC1*低発現マウスが第2世代目までにDKCの表現型が再現されるのに対して，*TERC*や*TERT*のknockoutマウスでは1世代ごとにテロメアの短縮が認められ，世代が進むにつれて前者では精子形成の欠損，造血細胞の増殖障害などを，後者では消化管粘膜上皮のアポトーシスなどが認められるようになるが，DKCの表現型は示さない[6,8,24]。

しかし一方で，*TERT*の変異を有するHHSの表現型を示す症例が存在しており，これらの遺伝子変異の部位や両アレルの変異の存在などがDKCの表現型に関与している可能性がある[25]。また，*TERC*の変異が認められるDKCの家系においては，世代が進むにつれて発症年齢が早まり，テロメア長の短縮も顕著になってくる世代促進現象が認められる[26]。このことは前述のマウスモデルでも同様の結果が得られており，DKCの表現型には世代の促進が重要な役割をしていると予想される[18,24]。そして，Fanconi貧血などの他の遺伝性骨髄不全症の発症年齢中央値が10歳以下なのに対して，DKCは15歳前後で，半数近くの症例が成人で診断されていることから，世代促進だけでなく加齢もDKCの表現型に重要な役割をしていると予想される（図3）[27]。

2）*TINF2*遺伝子変異

近年，染色体14q11.2上に存在する*TINF2*の変異が常染色体優性遺伝型のDKCで同定された[28,29]。*TINF2*はShelterin複合体を構成するTIN2をコードしている[30]。テロメアDNAの最末端部位は，DNAの3'末端が突出（オーバーハング）して一本鎖になっている。また，哺乳類のテロメアは折り曲がってTループと呼ばれる構造を

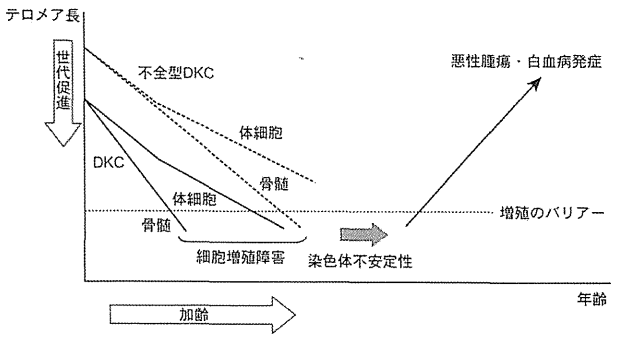

図3　DKCの発症機序

DKCはテロメア関連遺伝子変異によるテロメア伸長補正の障害，世代促進，加齢が病態の形成に重要である。テロメア関連遺伝子変異のテロメア補正の障害が軽度の場合や，世代促進や加齢が進んでいない場合は，DKCの特徴的身体所見が出現しないで不全型DKCを発症する可能性がある。

（筆者作成）

scaRNAs (small Cajalbody RNAs 蛋白)　RT (reverse transcriptase)

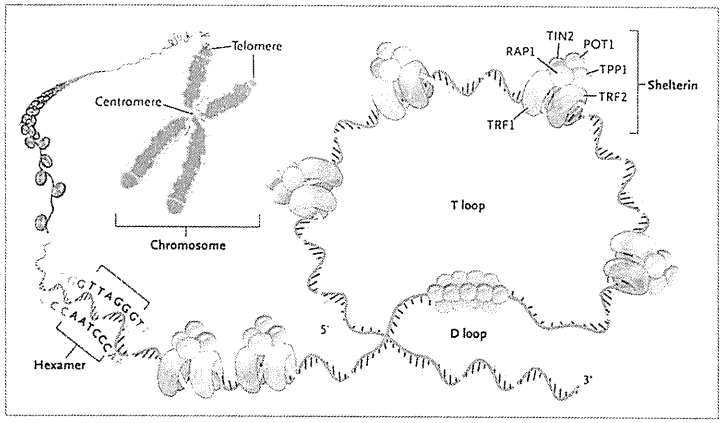

図4　Shelterin 複合体

テロメア DNA の最末端部位は，DNA の 3' 末端が突出（オーバーハング）して一本鎖になっている。また，哺乳類のテロメアは折り曲がってTループと呼ばれる構造をとり，このオーバーハングした一本鎖 DNA は，その上流のテロメア二本鎖の中に入り込みDループを構成する。Shelterin 複合体は，この特異的な構造形成や保護などを行っている。（文献9より改変）

とり，このオーバーハングした一本鎖 DNA はその上流のテロメア二本鎖の中に入り込み，Dループを構成する[30]。Shelterin 複合体はこの特異的な構造形成や保護などを行っているが，Shelterin 複合体は二本鎖 DNA と結合する TRF1 と TRF2，一本鎖 DNA に結合する POT1，これらの蛋白を結合させ複合体を形成する役割をもつ TIN2，RAP1，TPP1 で構成されている（図4）[30]。

TINF2 の変異は DKC の約 10 ～ 15%に認められ，DKC1 の次に多く認められる遺伝子変異である[7]。*TINF2* の変異の多くはヘテロの point mutation で，半数以上が TRF1 との結合ドメインの中のコドン 282arginine の変異である。また，その他の変異の大多数もコドン 282 近傍の変異であり，この領域が *TINF2* の機能として重要であることを示唆している。*TINF2* の変異の機能に関しては不明な点が多くあるが，*TINF2* の knock out マウスは胎性致死となることから，*TINF2* は細胞の生存に必須の蛋白であることが予想される[31]。また，*TINF2* の conservation region の変異は，TRF1 との結合ができなくなることで Shelterin 複合体の機能が障害されるのではないかと予想されている[32]。

4．常染色体劣性型の DKC

常染色体劣性遺伝型の DKC の頻度は少なく，全体の 1～2%にしか認められない[7]。これまでに原因遺伝子としては，前述の *TERT* や snoRNA である *NOP10*，*NHP2* が同定されている（表1）[7, 14]。常染色体劣性遺伝型の DKC に認められた *TERT* の変異は，RT ドメインの中に位置する R811C と R901W のホモ変異である[25]。これらの変異の機能は haploinsufficiency 効果でテロメラーゼ活性を減弱させるが，ホモ変異であるためテロメラーゼ活性の減弱が強く，DKC や HHS の表現型を示す。しかし，これらの *TERT* 変異の DKC 発症形式が常染色体劣性遺伝型かは不明瞭で，R811C 症例のヘテロの変異を有する両親は軽度ではあるが DKC の表現型とも考えられる症候を有しており，世代促進が進んでいないために DKC の表現型が出ていないだけかもしれない。

NOP10 や NHP2 は，Dyskerin などと snoRNA 複合体を形成し，*TERC* の boxH/ACA ドメインと結合し，テロメラーゼ複合体の processing と安定化の役割を果たしている[14, 20]。これまでに *NOP10* はホモ変異が，*NHP2* はホモ変異と両アレル変異が認められているが，これらの変異によって *TERC* の発現が減少し，テロメラーゼ活性が減弱することで DKC が発症すると考えられている[33, 34]。

近年，既知の原因遺伝子に変異を認めない DKC 2症例において，テロメラーゼ複合体のホロ酵素である *TCAB1* に両アレルの遺伝子変異が発見された[10]。*TCAB1* は *TERC* と CAB box を介して結合し核内の Cajalbody に移行させ，Dyskerin や他の scaRNAs を Cajalbody に集積させることでテロメラーゼ複合体の processing を進める機能があると考えられている。この *TCAB1* のヘテロ変異を有する家族が DKC の表現型を示していないことや，*in vitro* での機能解析結果から，*TCAB1* は常染色体劣性型の DKC の原因遺伝子と考えられている[10]。

5．不全型の DKC

成人になって特徴的身体所見を伴わず緩徐に発症する，不全型の DKC の存在が明らかになった[35]。不全型の DKC は，臨床的には再生不良性貧血や骨髄異形成症候群などと診断されていることが多く[35, 37]，本邦においても再生不良性貧血や骨髄異形成症候群の不応性貧血などの骨髄不全症の2～5%に不全型の DKC が認められる[38～40]。不全型の DKC の原因遺伝子としては，*TERC*，*TERT*，*TINF2* の報告があるが，前述のように *TERC*，*TERT* の変異は haploinsufficiency 効果を示し，テロメラーゼ活性の減弱の程度は弱いため，DKC の表現型となるには世代促進や加齢が必要となることがある。こうした変異の場合は，世代の早い症例では DKC の表現型が軽度で，不全型 DKC として診断されるのではないかと予想する（図3）。

これまでは再生不良性貧血の約 1/3 の症例はテロメア長が短縮し，再生不良性貧血の重症度，免疫抑制療法への不応性との関連が示唆されていたが[41～43]，これらは不全型 DKC の存在が明らかになる以前の検討で，再生不良性貧血とテロメア長の短縮化が再生不良性貧血の病態にどのように関与しているかは明らかではない。しかし不全型の DKC は，効果の得られない免疫抑制療法が行われたり，血縁間同種造血幹細胞移植の際に健常人と区別が困難な軽症の不全型 DKC 同胞がドナーとして選ばれたりすることがあるため，臨床的に診断を明確にすることは大変重要である[38～40]。こうした不全型の DKC をスクリーニングするのに，骨髄不全症の診断時にテロメア長の測定をすることは有用であると考える。

6．早老症とテロメア

早老症はウェルナー症候群（WS：Werner Syndrome）やハッチンソン・ギルフォード・プロジェリア症候群（HGPS：Hutchinson-Gilford Proge-

WS（Werner Syndrome；ウェルナー症候群）
HGPS（Hutchinson-Gilford Progeria Syndrome；ハッチンソン・ギルフォード・プロジェリア症候群）

ria Syndrome）に代表される加齢促進状態をもたらす遺伝性疾患である[44]。臨床症状としては，若年時より皮膚の萎縮や骨粗しょう症などの通常の加齢現象が出現し，心血管障害や悪性腫瘍の発生が高率に認められる。

近年，早老症の一つと考えられているロスモンド・トムソン症候群（RTS：Rothmund Thomson Syndrome）や，poikiloderma with neutropenia（PN）の原因遺伝子の一つである *C16orf57* の変異が臨床的にDKCと診断された症例で発見された[45]。RTSやPNは，DKCと共通する特徴的身体的所見を多く認めることから，これらの疾患がオーバーラップするような症例の存在が示唆されている。しかし，*C16orf57* の変異を認めたDKC症例は，末梢血テロメア長の短縮が認められていない。このことは，従来のテロメア長短縮化によって発症するDKCとは異なる発症機序のDKCの存在を示唆している。

また，WSの原因遺伝子である *WS* 遺伝子や，HGPSの原因遺伝子である *LMNA* 遺伝子には，テロメア長を制御する機能がある。WSやHGPSでは皮膚や筋肉のテロメア長の短縮化を認めるが，血球系では *WS* 遺伝子や *LMNA* 遺伝子の発現がないため，テロメア長の短縮化は認められない[46, 47]。このことは，血液系，皮膚，毛根，筋肉など，それぞれ分化した細胞には特有のテロメア制御機構が存在することを示唆している。もしかしたら，前述の不全型DKCは，血球系のテロメア制御にのみ関与する未知の機序の存在を示唆しているかもしれない。

7．DKCの治療

現在のところ，DKCの根本的治療は開発されていない。DKCの主な死因は，造血障害に伴う様々な合併症と，晩期の悪性腫瘍によるものが大多数である[7, 12]。これまで前者に対しては造血幹細胞移植（stem cell transplantation：SCT）が試みられてきたが，通常の骨髄破壊的前処置によるSCTは，移植後の肺線維症などの肺合併症，消化管狭窄，肝中心静脈閉塞症などの治療関連毒性が強く，長期生存例は稀であった[48]。DKCにおいてSCTの治療関連毒性が強い理由は，皮膚，消化管，肺胞上皮などの幹細胞のテロメア伸長補正の障害による増殖障害があるためと予想されている[48]。その後，fludarabineをベースとした骨髄非破壊的前処置によるSCTでは，前述の治療関連毒性が軽減され，長期の生存例も認められるようになった[48～50]。しかし，前述のようにDKCはHHSから不全型のDKCまでその表現型は様々で，どのような症例に対してどの時期にどのようにしてSCTを行うかといった臨床的な適応は明らかになっていない。また，他の後天的な骨髄不全症に対するSCTに比べて，DKCに対してのSCTは晩期の悪性腫瘍の合併がより高率となる可能性もあり，今後の症例の蓄積が必要である。

DKCの骨髄不全症に対しての保存的治療として，以前よりanabolic steroidやG-CSFなどの有効性が報告されてきた[7, 51, 52]。特に，anabolic steroidであるoxymetholone（0.5～5 mg/kg/day）の治療によって，約2/3の症例で血液学的な何らかの有効性が認められたとされている。これまでanabolic steroidによるDKCの血液学的な改善の機序は不明であったが，近年，*TERT* のpromoter領域にエストロゲン結合領域が認められ，アンドロゲンやエストロゲンなどの性ホルモンがテロメラーゼ活性を亢進させることが示された[53]。このことから，成人以降で診断された不全型のDKCに対しても，anabolic steroidなどによる治療は有効であると思われる。

RTS（Rothmund Thomson Syndrome；ロスモンド・トムソン症候群）　PN（poikiloderma with neutropenia）
SCT（stem cell transplantation；造血幹細胞移植）　iPS（induced pluripotent stem）

おわりに

DKCは，X連鎖劣性遺伝型の古典的なDKCが発見され，その原因がテロメアの機能不全であることが明らかになり，その後テロメアの機能不全という観点より，不全型のDKCの存在が明らかになってきた。しかし，依然として確立した治療法はなく，さらなる病態の解析による新たな治療法の確立が期待される。最近になり，再プログラム化されたDKC由来のinduced pluripotent stem（iPS）細胞において，OCT4やNANOGといった分化増殖万能性の維持に必須の転写因子が *TERC* や *DKC1* の発現を亢進させ，DKC由来のテロメラーゼ複合体の機能障害を克服し，テロメアの再伸長が認められた[54]。このことは，DKC由来のiPS細胞はテロメア関連遺伝子変異によるテロメア伸長の機能障害があってもテロメア伸長が回復することを示しており，将来の治療法の開発に発展するものと期待する。

文　献

1) O' Sullivan RJ, Karlseder J：Telomeres：protecting chromosomes against genome instability. Nat Rev Mol Cell Biol **11** (3)：171-181, 2010.
2) Harley CB, Futcher AB, Greider CW：Telomeres shorten during ageing of human fibroblasts. Nature **345**：458-460, 1990.
3) Harley CB, Vaziri H, Allsopp RC, et al：The telomere hypothesis of cellular aging. Exp Gerontol **27**：375-382, 1992.
4) Watson JD：Origin of concatemeric T7 DNA. Nat New Biol **239**：197-201, 1972.
5) Olovnikov AM：A theory of marginotomy. The incomplete copying of template margin in enzymic synthesis of polynucleotides and biological significance of the phenomenon. J Theor Biol **41**：181-190, 1973.
6) Calado RT, Young NS：Telomere maintenance and human bone marrow failure. Blood **111** (9)：4446-4455, 2008.
7) Walne AJ, Dokal I：Advances in the understanding of dyskeratosis congenita. Br J Haematol **145** (2)：164-172, 2009.
8) Carroll KA, Ly H：Telomere dysfunction in human diseases：the long and short of it! Int J Clin Exp Pathol **2**：528-543, 2009.
9) Calado RT, Young NS：Telomere diseases. N Engl J Med **361** (24)：2353-2365, 2009.
10) Zhong F, Savage SA, Shkreli M, et al：Disruption of telomerase trafficking by TCAB1 mutation causes dyskeratosis congenita. Genes Dev **25** (1)：11-16, 2011.
11) Vulliamy TJ, Marrone A, Knight SW, et al：Mutations in dyskeratosis congenita：their impact on telomere length and the diversity of clinical presentation. Blood **107**：2680-2685, 2006.
12) Dokal I：Dyskeratosis congenita in all its forms. Br J Haematol **110** (4)：768-779, 2000.
13) Marrone A, Dokal I：Dyskeratosis congenita：molecular insights into telomerase function, ageing and cancer. Expert Rev Mol Med **6** (26)：1-23, 2004.
14) Filipowicz W, Pogacic V：Biogenesis of small nucleolar ribonucleoproteins. Curr Opin Cell Biol **14** (3)：319-327, 2002.
15) He J, Navarrete S, Jasinski M, et al：Targeted disruption of Dkc1, the gene mutated in X-linked dyskeratosis congenita, causes embryonic lethality in mice. Oncogene **21**：7740-7744, 2002.
16) Mochizuki Y, He J, Kulkarni S, et al：Mouse dyskerin mutations affect accumulation of telomerase RNA and small nucleolar RNA, telomerase activity, and ribosomal RNA processing. Proc Natl Acad Sci U S A **101**：10756-10761, 2004.
17) Salowsky R, Heiss NS, Benner A, et al：Basal transcription activity of the dyskeratosis congenita gene is mediated by Sp1 and Sp3 and a patient mutation in a Sp1 binding site is associated with decreased promoter activity. Gene **293**：9-19, 2002.
18) Ruggero D, Grisendi S, Piazza F, et al：Dyskeratosis congenita and cancer in mice deficient in ribosomal RNA modification. Science **299**：259-262, 2003.

19) Cong YS, Wright WE, Shay JW : Human telomerase and its regulation. Microbiol Mol Biol Rev **66** (3) : 407-425, 2002.
20) Chen JL, Greider CW : Telomerase RNA structure and function : implications for dyskeratosis congenita. Trends Biochem Sci **29** : 183-192, 2004.
21) Xin ZT, Beauchamp AD, Calado RT, et al : Functional characterization of natural telomerase mutations found in patients with hematologic disorders. Blood **109** (2) : 524-532, 2007.
22) Marrone A, Stevens D, Vulliamy T, et al : Heterozygous telomerase RNA mutations found in dyskeratosis congenita and aplastic anemia reduce telomerase activity via haploinsufficiency. Blood **104** : 3936-3942, 2004.
23) Ly H, Calado RT, Allard P, et al : Functional characterization of telomerase RNA variants found in patients with hematologic disorders. Blood **105** : 2332-2339, 2005.
24) Cheong C, Hong KU, Lee HW : Mouse models for telomere and telomerase biology. Exp Mol Med **35** : 141-153, 2003.
25) Marrone A, Walne A, Tamary H, et al : Telomerase reverse-transcriptase homozygous mutations in autosomal recessive dyskeratosis congenita and Hoyeraal-Hreidarsson syndrome. Blood **110** (13) : 4198-4205, 2007.
26) Vulliamy T, Marrone A, Szydlo R, et al : Disease anticipation is associated with progressive telomere shortening in families with dyskeratosis congenita due to mutations in TERC. Nat Genet **36** : 447-449, 2004.
27) Alter BP : Diagnosis, genetics, and management of inherited bone marrow failure syndromes. Hematology Am Soc Hematol Educ Program : 29-39, 2007.
28) Savage SA, Giri N, Alter BP, et al : TINF2, a component of the shelterin telomere protection complex, is mutated in dyskeratosis congenita. Am J Hum Genet **82** (2) : 501-509, 2008.
29) Walne AJ, Vulliamy T, Dokal I, et al : TINF2 mutations result in very short telomeres : analysis of a large cohort of patients with dyskeratosis congenita and related bone marrow failure syndromes. Blood **112** (9) : 3594-3600, 2008.
30) de Lange T : Shelterin : the protein complex that shapes and safeguards human telomeres. Genes Dev **19** (18) : 2100-2110, 2005.
31) Chiang YJ, Kim S-H, Hodes RJ, et al : Telomere-Associated Protein TIN2 Is Essential for Early Embryonic Development through a Telomerase-Independent Pathway. Mol Cell Biol **24** : 6631-6634, 2004.
32) Kim SH, Davalos AR, Beausejour C, et al : Telomere dysfunction and cell survival : roles for distinct TIN2-containing complexes. J Cell Biol **181** (3) : 447-460, 2008.
33) Walne AJ, Vulliamy T, Marrone A, et al : Genetic heterogeneity in autosomal recessive dyskeratosis congenita with one subtype due to mutations in the telomerase-associated protein NOP10. Hum Mol Genet **16** : 1619-1629, 2007.
34) Vulliamy T, Beswick R, Kirwan M, et al : Mutations in the telomerase component NHP2 cause the premature ageing syndrome dyskeratosis congenita. Proc Natl Acad Sci U S A **105** (23) : 8073-8078, 2008.
35) Fogarty PF, Yamaguchi H, Wiestner A, et al : Late presentation of dyskeratosis congenita as apparently acquired aplastic anaemia due to mutations in telomerase RNA. Lancet **362** : 1628-1630, 2003.
36) Yamaguchi H, Baerlocher GM, Lansdorp PM, et al : Mutations of the human telomerase RNA gene (TERC) in aplastic anemia and myelodysplastic syndrome. Blood **102** (3) : 916-918, 2003.
37) Yamaguchi H, Calado RT, Ly H, et al : Mutations in TERT, the gene for telomerase reverse transcriptase, in aplastic anemia. N Engl J Med **352** : 1413-1424, 2005.
38) Liang J, Yagasaki H, Kamachi Y, et al : Mutations in telomerase catalytic protein in Japanese children with aplastic anemia. Haematologica **91** : 656-658, 2006.
39) Takeuchi J, Ly H, Yamaguchi H, et al : Identification and functional characterization of novel telomerase variant alleles in Japanese patients with bone-marrow failure syndromes. Blood Cells Mol Dis **40** : 185-191, 2008.

40) Yamaguchi H, Inokuchi K, Takeuchi J, et al : Identification of TINF2 gene mutations in adult Japanese patients with acquired bone marrow failure syndromes. Br J Haematol **150** : 725-727, 2010.
41) Ball SE, Gibson FM, Rizzo S, et al : Progressive telomere shortening in aplastic anemia. Blood **91** (10) : 3582-3592, 1998.
42) Brummendorf TH, Maciejewski JP, Mak J, et al : Telomere length in leukocyte subpopulations of patients with aplastic anemia. Blood **97** (4) : 895-900, 2001.
43) Lee JJ, Kook H, Chung IJ, et al : Telomere length changes in patients with aplastic anaemia. Br J Haematol **112** (4) : 1025-1030, 2001.
44) Martin GM : Genetic modulation of senescent phenotypes in Homo sapiens. Cell **120** (4) : 523-532, 2005.
45) Walne AJ, Vulliamy T, Beswick R, et al : Mutations in C16orf57 and normal-length telomeres unify a subset of patients with dyskeratosis congenita, poikiloderma with neutropenia and Rothmund-Thomson syndrome. Hum Mol Genet **19** (22) : 4453-4461, 2010.
46) Decker ML, Chavez E, Vulto I, et al : Telomere length in Hutchinson-Gilford progeria syndrome. Mech Ageing Dev **130** (6) : 377-383, 2009.
47) Ishikawa N, Nakamura K, Izumiyama-Shimomura N, et al : Accelerated *in vivo* epidermal telomere loss in Werner syndrome. Aging **3** (4) : 417-429, 2011.
48) Ostronoff F, Ostronoff M, Calixto R, et al : Fludarabine, cyclophosphamide, and antithymocyte globulin for a patient with dyskeratosis congenita and severe bone marrow failure. Biol Blood Marrow Transplant **13** (3) : 366-368, 2007.
49) de la Fuente J, Dokal I : Dyskeratosis congenita : advances in the understanding of the telomerase defect and the role of stem cell transplantation. Pediatr Transplant **11** (6) : 584-594, 2007.
50) Coman D, Herbert A, Hallahan A, et al : Unrelated cord blood transplantation in a girl with Hoyeraal-Hreidarsson syndrome. Bone Marrow Transplant **42** (4) : 293-294, 2008.
51) Bayne S, Liu JP : Hormones and growth factors regulate telomerase activity in ageing and cancer. Mol Cell Endocrinol **240** : 11-22, 2005.
52) Erduran E, Hacisalihoglu S, Ozoran Y : Treatment of dyskeratosis congenita with granulocyte-macrophage colony-stimulating factor and erythropoietin. J Pediatr Hematol Oncol **25** (4) : 333-335, 2003.
53) Calado RT, Yewdell WT, Wilkerson KL, et al : Sex hormones, acting on the TERT gene, increase telomerase activity in human primary hematopoietic cells. Blood **114** (11) : 2236-2243, 2009.
54) Agarwal S, Loh YH, McLoughlin EM, et al : Telomere elongation in induced pluripotent stem cells from dyskeratosis congenita patients. Nature **464** (7286) : 292-296, 2010.

Pediatr Transplantation 2012: 16: 340–345

Pediatric Transplantation
DOI: 10.1111/j.1399-3046.2012.01669.x

Matched sibling donor stem cell transplantation for Fanconi anemia patients with T-cell somatic mosaicism

Yabe M, Shimizu T, Morimoto T, Koike T, Takakura H, Tsukamoto H, Muroi K, Oshima K, Asami K, Takata M, Yamashita T, Kato S, Yabe H. Matched sibling donor stem cell transplantation for Fanconi anemia patients with T-cell somatic mosaicism.

Abstract: SCT from HLA-identical sibling donors is generally associated with an excellent survival in FA patients if performed prior to the development of MDS or leukemia. However, the optimal conditioning regimen has not been defined. We report here our experience with 15 Japanese FA patients who underwent HLA-matched sibling donor SCT. The aim of this study is to compare radiation-based conditioning to Flu-based conditioning for FA patients in a Japanese population where the T-cell somatic mosaicism is higher than in the Caucasian population. Eight patients (a-group) received a radiation-based conditioning (500–600 cGy of thoracoabdominal/TBI) with CY dose modification (20–120 mg/kg), and ATG; two patients exhibited rejection. Seven patients (b-group) received CY (40 mg/kg), 150–180 mg/m^2 of Flu, and ATG. Durable engraftment was demonstrated in all patients. In FA patients, Flu-based conditioning may allow stable engraftment in matched sibling donor transplantation without radiation, even in patients with T-cell somatic mosaicism.

Miharu Yabe[1], Takashi Shimizu[2], Tsuyoshi Morimoto[2], Takashi Koike[2], Hiromitsu Takakura[2], Hideo Tsukamoto[3], Kazuo Muroi[4], Koichi Oshima[5], Keiko Asami[6], Minoru Takata[7], Takayuki Yamashita[8], Shunichi Kato[1] and Hiromasa Yabe[1]

[1]Department of Cell Transplantation, [2]Department of Pediatrics, and [3]Teaching and Research Support Center, Tokai University Hospital, Kanagawa, [4]Division of Cell Transplantation and Transfusion, Jichi Medical School, Tochigi, [5]Division of Hematology and Oncology, Saitama Children's Medical Center, Saitama, [6]Department of Pediatrics, Niigata Cancer Center, Niigata, [7]Laboratory of DNA Damage Signaling, Department of Late Effect Studies, Radiation Biology Center, Kyoto University, Kyoto, [8]Laboratory of Molecular Genetics, The Institute for Molecular and Cellular Regulation, Gunma University, Gunma, Japan

Key words: Fanconi anemia – stem cell transplantation – HLA-matched sibling donors – fludarabine – T-cell somatic mosaicism

Miharu Yabe, MD, Department of Cell Transplantation, Tokai University Hospital, Shimokasuya 143, Isehara, Kanagawa 259-1193, Japan
Tel.: 81 463 93 1121
Fax: 81 463 93 8607
E-mail: miharu@is.icc.u-tokai.ac.jp

Accepted for publication 11 January 2012

Somatic mosaicism, the presence of non-FA cells among FA hematopoietic cells, has been considered a risk factor for engraftment in SCT from alternative donors, because DEB-resistant T-cells may increase the risk of graft rejection (1). Wagner et al. (2) reported that engraftment was poorer in unrelated donor recipients with T-cell somatic mosaicism not treated with a Flu-containing regimen. We reported that there is a high frequency of T-cell somatic mosaicism in Japanese FA patients (3). The current study presents the results of matched sibling donor SCT in 15 FA patients undergoing two types of conditioning regimens: radiation-based conditioning with CY dose modification and Flu-based regimen without radiation.

Abbreviations: ALG, antilymphocyte globulin; ATG, antithymocyte globulin; BMT, bone marrow transplantation; CsA, cyclosporine A; CY, cyclophosphamide; DEB, diepoxybutane; FA, Fanconi anemia; Flu, fludarabine; GVHD, graft-vs.-host disease; HLA, human leukocyte antigen; INFA, International Fanconi Anemia Registry; MDS, myelodysplastic syndrome; MMC, mitomycin-C; MTX, methotrexate; RA, refractory anemia; RRT, regimen-related toxicity; SCT, stem cell transplantation; TAI, thoracoabdominal irradiation; TBI, total body irradiation.

Patients and methods

Patients and donor selection

Between 1987 and 2008, 15 patients with FA received 17 SCTs from their HLA-matched sibling donors. The diagnosis of FA was confirmed by chromosomal breakages induced by MMC or 0.1 μg/mL DEB. The chromosomal fragility test for CY metabolites was performed using the serum obtained from other CY-treated, non-FA SCT patients with severe aplastic anemia as previously described (4). We chose the concentration of 0.4 μg/mL for CY metabolites in chromosomal fragility testing of FA patients because it induces multiple chromosomal breaks in FA patients while having little clastogenic effect on normal cells (4). Peripheral lymphocytes from 78 FA patients underwent both CY metabolite and DEB tests in our laboratory. Patients with 50% or more cells insensitive to treatment with 0.1 μg/mL DEB and/or 0.4 μg/mL CY metabolite were classified as high-mosaic in this study for comparison with patients in the IFAR (5). Patient characteristics are shown in Table 1. Age at transplant ranged from 5 to 24 yr. Twelve patients had severe aplastic anemia, and three had RA. Determination of complementation groups was informative in 11 patients, of whom six were placed in group A and five in group C. Of our 15 patients, seven had received androgen therapy, and all 15 were transfusion-dependent at the time of SCT. All 15 donors (14 bone marrow, one cord blood for patient 8) had negative results of DEB/MMC test prior to transplant and were matched (at HLA loci A, B, and DR) to HLA-identical siblings. Harvested marrow was not manipulated.

Conditioning regimen and GVHD prophylaxis

The conditioning regimen of eight patients of a-group (Nos. 1–8) consisted of the following: modified CY (20–120 mg/kg), either TAI (500–600 cGy) or TBI, and ATG or ALG. We provisionally reduced the dose of CY according to the increase of chromosomal breaks case by case, although we set a minimum dose of 20 mg/kg.

Since 2000, Flu – an antimetabolite and immunosuppressive agent – has been used as a part of conditioning. The regimen of seven patients of b-group (Nos. 9–15) included CY (40 mg/kg), Flu (150–180 mg/m^2), and ATG, without radiation. GVHD prophylaxis was carried out using CsA; short-term MTX (15 mg/m^2 on day 1; 10 mg/m^2 on days 3, 5, and 11) administration was utilized in patients older than 10 yr.

Analysis of chimerism

Engraftment on the bone marrow was assayed using short tandem repeats analysis, XY chromosomal analysis, or fluorescence *in situ* hybridization with XY chromosome-specific probes.

The Tokai University Hospital institutional review board approved the collection and reporting of these data.

Results

Chromosomal fragility test

Table 2 shows a summary of the results of cytogenetic testing of 78 FA patients; there was a linear correlation between the percentage of aberrant metaphases in lymphocytes treated with CY metabolites and the percentage in lymphocytes treated with DEB ($r = 0.868$) (Fig. 1). Among the 12 patients tested for DEB, four were shown to be high-mosaic: two in a-group and two in b-group (Table 1). In the CY metabolite test, eight of 15 patients (four in each group) were shown to have high-mosaic.

Table 1. Patient characteristics; (a) radiation-based conditioning with CY dose modification group; (b) fludarabine-based conditioning without radiation group

No.	Age at SCT (yr)	Sex	Status at SCT (% blasts)	Clonal abnormality	Complementation group	CY test	CY mosaic (%)	DEB mosaic (%)	Prior therapy	No. of prior blood transfusions
(a)										
1	8	F	SAA (0)	No	A	0.16	91.0	56.0	PSL, Androgen	>20
2	6	M	SAA (0)	No	C	0.43	73.2	NT	None	1–20
3	14	M	SAA (0)	No	C	0.44	79.4	NT	Androgen	1–20
4	11	M	SAA (0)	No	Unknown	0.23	77.0	NT	PSL	1–20
5	5	M	SAA (0)	No	C	1.12	47.0	34.0	GCSF, Epo, CsA	1–20
6	10	M	SAA (0)	No	C	2.85	20.0	13.3	PSL, Androgen	1–20
7	24	F	RA (<5)	del(7)(p12)	Unknown	2.66	1.0	0	PSL, CsA, Androgen	1–20
8	5	F	RA (<5)	No	C	0.96	49.5	56.0	PSL, Androgen	1–20
(b)										
9	8	F	SAA (0)	No	A	0.52	58.0	54.0	None	1–20
10	15	F	SAA (0)	No	Unknown	0.81	50.0	8.0	None	1–20
11	6	M	SAA (0)	No	Unknown	2.91	13.0	4.9	Androgen	1–20
12	6	M	SAA (0)	No	A	1.05	27.0	17.0	Androgen	1–20
13	1	M	RA (<5)	Add(2)(q33)	A	0.20	82.0	63.0	None	>20
14	9	F	SAA (0)	No	A	0.61	66.0	16.0	None	1–20
15	4	F	SAA (0)	No	A	2.60	15.0	3.0	None	>20

F, female; M, male; SAA, severe aplastic anemia; CY test, cyclophosphamide metabolites-induced (0.4 μg/mL) test, with results listed as mean number of chromosome breaks per cell; CY mosaic, percentage of cells with 0.4 μg/mL cyclophosphamide metabolites-insensitivity; DEB mosaic, percentage of cells with 0.1 μg/mL diepoxybutane insensitivity; NT, not tested; PSL, prednisolone; GCSF, granulocyte colony-stimulating factor; Epo, erythropoietin.

Table 2. Chromosome fragility test performed with DEB and CY metabolites in 78 FA patients

Agent	Breaks/cell, *n*	Aberrant cells, %	Aberrations/aberrant cell, *n*
Spontaneous	0.0 6 ± 0.09 (0–0.49)	7.93 ± 10.63 (0–66)	1.04 ± 0.16 (1–2)
DEB (0.1 μg/mL)	3.10 ± 2.67 (0.03–12.0)	68.63 ± 27.64 (2–100)	3.85 ± 2.37 (1–12)
CY metabolites (0.4 μg/mL)	1.38 ± 1.16 (0–5.57)	54.91 ± 24.61 (1–100)	2.20 ± 1.02 (1–5.93)

DEB, diepoxybutane; CY, cyclophosphamide, FA, Fanconi anemia.

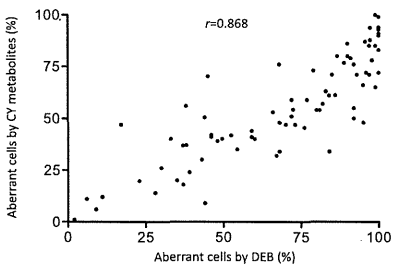

Fig. 1. Linear correlation between the percentage of aberrant metaphases in lymphocytes treated with 0.4 μg/mL CY metabolites and the percentage in lymphocytes treated with 0.1 μg/mL-DEB.

Engraftment and chimerism

The transplantation characteristics and the follow-up characteristics after transplantation are summarized in Table 3 and 4, respectively. Seven of eight patients in a-group engrafted. Patient 1, who was high-mosaic with 56% DEB-insensitive and 91% CY metabolites-insensitive lymphocytes, did not engraft; this patient received an infusion of marrow cells from another HLA-matched sibling after a conditioning regimen of TBI (8 Gy) + CY (150 mg/kg) + ALG, and engrafted. Patient 7 achieved successful engraftment after receiving 20 ng/kg of CY without any RRT. Although she was not high-mosaic, she developed late graft rejection on day 205 after pure red cell aplasia. Chromosomal analysis of peripheral blood cultured with phytohemagglutinin and that of bone marrow showed mixed chimerism. She received a second BMT from the same brother on day 240 after TBI (7.5 Gy) + CY (60 mg/kg) + ALG, and successfully engrafted.

Successful engraftment was achieved in all seven patients in b-group, independent of the proportion of DEB- or CY-insensitive cells

Table 3. Transplantation characteristics; (a) radiation-based conditioning with CY dose modification group; (b) fludarabine-based conditioning without radiation group

No.	Conditioning	TNC/kg (×10⁸)	Engraftment: Day ANC >0.5 × 10⁹/L	Engraftment: Day platelet >50 × 10⁹/L	Organ toxicity (Bearman) Grade I/II	GVHD: Acute	GVHD: Chronic
(a)							
1-1	CY(40)* + TAI(6) + ALG	4.7	Rejection	Rejection	No	NE	NE
1-2	CY(150) + TBI(8) + ALG	4.5	21	74	Stomatitis, mucositis	0	Lim
2	CY(40) + TAI(6) + ALG	4.5	27	22	Stomatitis	0	–
3	CY(45) + TAI(6) + ALG	2.5	12	27	Stomatitis	0	Lim
4	CY(120) + TAI(6) + ALG	1.7	13	26	No	0	–
5	CY(20) + TAI(6)	6.6	16	21	No	0	–
6	CY(20) + TAI(6) + ATG	3.1	17	33	No	0	–
7-1	CY(20) + TAI(5) + ALG	≥2.0	14/No	16/No	No	0	–
7-2	CY(60) + TBI(7.5) + ALG	≥2.0	15	Unknown/Yes	Stomatitis, liver	II	Ext
8	CY(40) + TBI(6) + ATG	0.21† CB	15	38	Stomatitis	0	–
(b)							
9	CY(40) + Flu(180) + ATG	6.2	10	12	No	0	–
10	CY(40) + Flu(150) + ATG	5.2	14	23	Stomatitis, liver	0	–
11	CY(40) + Flu(150) + ATG	3.5	14	31	Stomatitis	0	–
12	CY(40) + Flu(150) + ATG	3.3	11	24	No	0	–
13	CY(40) + Flu(150) + ALG	7.8	9	17	Stomatitis	0	–
14	CY(40) + Flu(150) + ATG	4.1	11	17	Stomatitis	0	–
15	CY(40) + Flu(150) + ATG	3.9	12	24	No	0	–

TNC, total nucleated cells; NE, not evaluable.
*The number in parentheses indicates the dose, and units are Gy for TAI and TBI, mg/m² for Flu, and mg/kg for CY.
†Post-thawing cell dose of cord blood.

Table 4. Follow-up characteristics after transplantation; (a) radiation-based conditioning with CY dose modification group; (b) fludarabine-based conditioning without radiation group

No.	Chimerism status (% donor cells): At the first time (source/days after SCT)	Chimerism status (% donor cells): At the last time (source/months after SCT)	Complication (months after SCT)	Outcome (months after SCT)
(a)				
1-1	NE	NE	Hepatitis B and C	Rejection. 2nd SCT
1-2	100 (BM/42)	NT	Ovarian dysfunction Hepatic carcinoma (145)	Dead/hepatic carcinoma (147)
2	100 (BM/41)	100 (PB/280)	Prediabetic state	Alive (280)
3	NT	NT	Tongue carcinoma (102)	Dead/tongue carcinoma (114)
4	NT	NT	No	Alive (250)
5	NT	NT	No	Alive (220)
6	100 (BM/14)	100 (BM/2)	No	Dead/accident (154)
7-1	100 (BM/15)	50 (PB/3)	Ovarian dysfunction	PRCA/late rejection, 2nd SCT (eight months)
7-2	100 (BM/15)	100 (PB/60)	Esophagus carcinoma (138) Tongue carcinoma (177)	Alive with cancer disease (234)
8	100 (PB/15)	100 (PB/178)	Pheochromocytoma (147) Prediabetic state	Alive (178)
(b)				
9	100 (BM/12)	100 (PB/105)	No	Alive (129)
10	100 (BM/32)	100 (PB/81)	No	Alive (117)
11	100 (BM/14)	100 (PB/60)	No	Alive (86)
12	98.8 (BM/14)	100 (PB/36)	No	Alive (48)
13	100 (BM/28)	100 (PB/17)	No	Alive (46)*
14	100 (BM/14)	100 (PB/46)	No	Alive (46)
15	100 (BM/14)	95 (PB/41)	No	Alive (41)

NE, not evaluable; BM, bone marrow; NT, not tested; PB, peripheral blood; PRCA, pure red cell aplasia.
*This case was reported by Oshima et al. (21).

(ranges, 3–63% and 13–82%, respectively). The time to an absolute neutrophil count (ANC) $>0.5 \times 10^9$/L was 9–14 days, and to a platelet count of 50×10^9/L was 12–31 days. In patients of b-group, chimerism of their BM mononuclear cells in the early stages after SCT was 98.8–100% of donor type. Although two of these seven patients showed transient mixed chimerism (patient 14 and 15) in the peripheral blood mononuclear cells during the first year after SCT, all patients achieved >95% donor chimerism.

Toxicity

The grade of toxicity was low both in two groups. None of the patients showed grade III/VI RRT (Bearman's criteria) at any evaluation point.

GVHD

Only one patient (patient 7) developed grade II acute GVHD after the second transplant, and chronic GVHD was observed in three patients who developed malignancies as late effects (patient 1, 3 and 7). No patients of b-group had acute and/or chronic GVHD.

Outcome

In patients of a-group, hepatocarcinoma and tongue/esophagus carcinoma were observed in patients 1 and 7, at 12 and 10/14 yr after BMT, respectively. Tongue carcinoma and pheochromocytoma were also observed in patients three and eight, at nine and 12 yr after BMT, respectively. Causes of death in a-group were solid cancer in two of eight, and one died of accident. Two patients suffered from ovarian dysfunction (patient 1 and 7), and two patients are in prediabetic state (patient 2 and 8). None of the b-group required a second SCT (median follow-up, 48 months; range, 41–129 months); all patients are alive with a Lansky/Karnofsky score of 100%, and there are no late side effects such as ovarian failure or other endocrinopathy.

Discussion

Graft rejection, RRT, and severe acute GVHD have been the major causes of SCT failure in FA patients. However, in FA patients, SCT from an HLA-identical sibling donor is generally associated with an excellent outcome when performed before leukemic transformation. The approach used by Gluckman et al. (6), including low-dose

CY (20–40 mg/kg) + TAI/TBI (400–450 cGy), has been the standard SCT conditioning regimen. This conditioning regimen provided good results, with >80% survival at 3–10 yr (7, 8). Non-radiation regimens have been increasingly used for FA patients to reduce the late effects associated with radiation, such as endocrinopathies, infertility, and cataracts.

Bonfim et al. (9) reported using only CY (60 mg/kg) in 43 patients from matched-related SCT donors; Ayas et al. (10) also reported using a CY (60 mg/kg) + ATG regimen without radiation in 34 patients with matched-related donor SCT. Overall survival rate in these studies were 93% (median follow-up, 3.7 yr) and 96.9% (median follow-up, 33.7 months), respectively. However, MacMillan et al. (1) observed a high rate of graft failure in FA patients receiving unrelated donor transplants with T-cell somatic mosaicism, suggesting that the presence of DEB-insensitive T-cells increased the risk of graft rejection.

We showed that there was a linear correlation between the percentage of aberrant metaphases in lymphocytes treated with CY metabolites and those treated with DEB (Fig. 1). On the basis of these data, we suggested that DEB-insensitive cells are also CY-insensitive cells. Therefore, incomplete ablation of DEB-resistant host lymphocytes might increase the risk of graft failure. If patients with 50% or more DEB-insensitive cells are classified as high-mosaic, only 10% of FA patients have been reported to exhibit >50% insensitive cells in IFAR patients (5); however, in our study, among the 78 patients, 24 were high-mosaic (30.8%). A conditioning regimen that exhibits strong cytotoxic activity against lymphocytes and minimized exposure to DNA cross-linking agents may be necessary for Japanese FA patients because the T-cell somatic mosaicism in Japanese population is higher than the Caucasian population. The patients in a-group received high-dose therapy, particularly those who received a second transplant. This might explain the high incidence of cancer. Furthermore, the two patients who developed tongue carcinoma in a-group had oral chronic GVHD. There was a significant association of the oral squamous cell carcinoma with chronic GVHD (11, 12).

In recent years, Flu-containing conditioning regimens for FA have become more popular and have been successfully employed, especially in SCT from alternative donors (2, 13, 14). Flu is an antimetabolite and immunosuppressive agent that is not a DNA cross-linking agent. The first FA patient with leukemic transformation successfully treated by matched sibling BMT following a Flu-based conditioning regimen was reported in 1997 (15). Flu is an attractive and tolerable agent for FA because it is not an alkylating agent and has an antileukemic effect. Furthermore, omission of irradiation from a conditioning regimen has been considered to reduce the late effects. Tan et al. (16) reported that 11 patients with 0–20% DEB-insensitive cells had received a conditioning regimen of CY (20 mg/kg) + Flu (175 mg/m^2) + ATG without irradiation, followed by an infusion of HLA-genotypically identical T-cell-depleted bone marrow or cord blood. Neutrophil engraftment was observed in all patients, but secondary graft failure was observed in one patient. No patients experienced severe RRT or either acute or chronic GVHD, and nine are alive and well at a median follow-up of 2.9 yr. Ertem et al. (17), who used a similar regimen (CY 20 mg/kg + Flu 150 mg/m^2 + ATG), reported successful engraftment in 6 FA patients. Stepensky et al. (18) also reported that a combination of Flu with ATG and low-dose CY without radiation was safe and demonstrated low rejection rates when compared with alternative regimens in patients with FA. After 2000, we selected Flu, a consistent, reduced dose of CY 40 mg/kg, and ATG without radiation as conditioning for HLA-matched sibling donor SCT, and successful engraftment was achieved in all seven patients with stable chimerism, independent of the T-cell somatic mosaicism. They are all disease free and in good clinical condition without any late side effects.

Age at SCT (>10 yr) is also a risk factor of acute GVHD (19). To prevent moderate-to-severe acute GVHD, we have used the combination of CsA plus short-term MTX in patients older than 10 yr in matched sibling donor SCT and used tacrolimus plus short-term MTX after alternative donor transplant (13). No patients had severe MTX toxicity, and none of them died of acute GVHD in either a- and b-group. Bonfim et al. (9) have also used CsA plus short-term MTX in HLA-matched related donor SCT in 43 FA patients. They found a very low incidence of acute GVHD and suggested that less regimen-related tissue damage enabled the delivery of all four scheduled MTX doses in the majority of patients; MTX dosing was previously shown to be important in controlling the incidence of GVHD (20). These combinations of GVHD prophylaxis including MTX considerably decreased the severe acute GVHD for FA patients, which could have varied in accordance with ethnic differences.

Our study indicates that a Flu-based regimen without radiation enabled successful engraftment

in HLA-matched sibling donor SCT even in FA patients with evidence of T-cell somatic mosaicism. It is very difficult to compare the outcome of two different regimens as there are two second transplant in a-group and the major differences between the follow-up times of two groups. Long-term follow-up and larger studies are warranted to confirm the high engraftment rates and reduction of post-transplant malignancies.

Acknowledgment

The authors thank Mr. Satoshi Arakawa, Mr. Yuzo Tanaka, and Miss Atsuko Masukawa in the central laboratory of Tokai University Hospital for their help with chromosomal analysis. We are indebted to Miss Ayako Tsuchida, Mr. Tatsuya Sugimoto, Miss Chie Nakashioya, and Osamu Hyodo in the Cell Transplantation center of Tokai University Hospital for chimerism analysis after the SCTs. This work was supported by a grant-in-aid from the Ministry of Education, Culture, Sports, Science, and Technology of Japan (No. 20591262) and a Research Grant for Intractable Diseases (H-21-061) from the Japanese Ministry of Health, Labor, and Welfare.

Disclosure

The authors declare no competing financial interests.

Author contributions

M. Yabe, H. Yabe: concept/design; M. Yabe, T. Shimizu, T. Morimoto, T. Koike, H. Takakura, H. Tsukamoto, K. Muroi, K. Asami, K. Oshima, M. Takata, T. Yamashita: data analysis/interpretation; S. Kato, H. Yabe: approval of the article.

References

1. Macmillan ML, Auerbach AD, Davies SM, et al. Haematopoietic cell transplantation in patients with Fanconi anaemia using alternative donors: Results of a total body irradiation dose escalation trial. Br J Haematol 2000: 109: 121–129.
2. Wagner JE, Eapen M, MacMillan ML, et al. Unrelated donor bone marrow transplantation for the treatment of Fanconi anemia. Blood 2007: 109: 2256–2262.
3. Yabe M, Yabe H, Hamanoue S, et al. In vitro effect of fludarabine, cyclophosphamide, and cytosine arabinoside on chromosome breakage in Fanconi anemia patients: Relevance to stem cell transplantation. Int J Hematol 2007: 85: 354–361.
4. Yabe M, Yabe H, Matsuda M, et al. Bone marrow transplantation for Fanconi anemia: Adjustment of the dose of cyclophosphamide for preconditioning. Am J Pediatr Hematol/Oncol 1993: 15: 377–382.
5. Auerbach AD. Fanconi anemia and its diagnosis. Mutat Res 2009: 668: 4–10.
6. Gluckman E, Berger R, Dutreix J. Bone marrow transplantation for Fanconi anemia. Semin Hematol 1984: 21: 20–26.
7. Dufour C, Rondelli R, Locatelli F, et al. Stem cell transplantation from HLA-matched related donor for Fanconi's anaemia: A retrospective review of the multicentric Italian experience on behalf of AIEOP-GITMO. Br J Haematol 2001: 112: 796–805.
8. Farzin A, Davies SM, Smith FO, et al. Matched sibling donor haematopoietic stem cell transplantation in Fanconi anaemia: An update of the Cincinnati children's experience. Br J Haematol 2007: 136: 633–640.
9. Bonfim CM, De Mederios CR, Bitencourt MA, et al. HLA-matched related donor hematopoietic cell transplantation in 43 patients with Fanconi anemia conditioned with 60 mg/kg of cyclophosphamide. Biol Blood Marrow Transplant 2007: 13: 1445–1460.
10. Ayas M, Al-Jrfri A, Al-Seraihi A, Elkum N, Al-Mahr M, El-Solh H. Matched related allogeneic stem cell transplantation in Saudi patients with Fanconi anemia: 10 year's experience. Bone Marrow Transplant 2008: 42: S45–S48.
11. Deeg HJ, Socié G, Schoch G, et al. Malignancies after marrow transplantation for aplastic anemia and Fanconi anemia: A joint Seattle and Paris analysis of results in 700 patients. Blood 1996: 87: 386–392.
12. Rosenberg PS, Socié G, Alter BP, Gluckman E. Risk of head and neck squamous cell cancer and death in patients with Fanconi anemia who did and did not receive tranplants. Blood 2005: 105: 67–73.
13. Yabe H, Inoue H, Matsumoto M, et al. Allogeneic haematopoietic cell transplantation from alternative donors with a conditioning regimen of low-dose irradiation, fludarabine and cyclophosphamide in Fanconi anaemia. Br J Haematol 2006: 134: 208–212.
14. Chaudhury S, Auerbach AD, Kernan NA, et al. Fludarabine-based cytoreductive regimen and T-cell-depleted grafts from alternative donors for the treatment of high-risk patients with Fanconi anaemia. Br J Haematol 2008: 140: 644–655.
15. Kapelushnik J, Or R, Slavin S, et al. A fludarabine-based protocol for bone marrow transplantation in Fanconi's anemia. Bone Marrow Transplant 1997: 20: 1109–1110.
16. Tan PL, Wagner JE, Auerbach AD, Deforte TE, Slungaard A, Macmillan ML. Successful engraftment without radiation after fludarabine-based regimen in Fanconi anemia patients undergoing genotypically identical donor hematopoietic cell transplantation. Pediatr Blood Cancer 2006: 46: 630–636.
17. Ertem M, Ileri T, Azik F, Uysal Z, Gozdasoglu S. Related donor hematopoietic stem cell transplantation for Fanconi anemia without radiation: A single center experience in Turkey. Pediatr Transplant 2009: 13: 88–95.
18. Stepensky P, Shapira MY, Balashov D, et al. Bone marrow transplanation for Fanconi anemia using fludarabine-based conditioning. Biol Blood Marrow Transplant 2011: 17: 1282–1288.
19. Neudrorf S, Sandes L, Kobrinsky N, et al. Allogeneic bone marrow transplantation for children with acute myelocytic anemia in first remission demonstrates a role for graft versus leukemia in the maintenance of disease-free survival. Blood 2004: 103: 3655–3661.
20. Nash RA, Pepe MS, Storb R, et al. Acute graft-versus-host disease: Analysis of risk factors after allogeneic marrow transplantation and prophylaxis with cyclosporine and methotrexate. Blood 1992: 80: 1838–845.
21. Oshima K, Kikuchi A, Mochizuki S, et al. Fanconi anemia in infancy: Report of hematopoietic stem cell transplantation to a 13-month-old patient. Int J Hematol 2009: 89: 722–723.

nature immunology

The kinase Btk negatively regulates the production of reactive oxygen species and stimulation-induced apoptosis in human neutrophils

Fumiko Honda[1], Hirotsugu Kano[2], Hirokazu Kanegane[3], Shigeaki Nonoyama[4], Eun-Sung Kim[5], Sang-Kyou Lee[5], Masatoshi Takagi[1], Shuki Mizutani[1] & Tomohiro Morio[1]

The function of the kinase Btk in neutrophil activation is largely unexplored. Here we found that Btk-deficient neutrophils had more production of reactive oxygen species (ROS) after engagement of Toll-like receptors (TLRs) or receptors for tumor-necrosis factor (TNF), which was associated with more apoptosis and was reversed by transduction of recombinant Btk. Btk-deficient neutrophils in the resting state showed hyperphosphorylation and activation of phosphatidylinositol-3-OH kinase (PI(3)K) and protein tyrosine kinases (PTKs) and were in a 'primed' state with plasma membrane–associated GTPase Rac2. In the absence of Btk, the adaptor Mal was associated with PI(3)K and PTKs at the plasma membrane, whereas in control resting neutrophils, Btk interacted with and confined Mal in the cytoplasm. Our data identify Btk as a critical gatekeeper of neutrophil responses.

Among 'professional' phagocytes with a sophisticated arsenal of microbicidal features, neutrophils are the dominant cells that mediate the earliest innate immune responses to microbes[1–3]. Neutrophils migrate to the site of infection, sense and engulf microorganisms, produce reactive oxygen species (ROS) and kill the invading microbes via ROS by acting together with antimicrobial proteins and peptides[1,2]. The enzyme responsible for the respiratory burst is NADPH oxidase, which catalyzes the production of superoxide from oxygen and NADPH. This enzyme is a multicomponent complex that consists of membrane-bound flavocytochrome b_{558} (gp91^{phox} and p22^{phox}), cytosolic components (p47^{phox}, p67^{phox} and p40^{phox}) and a GTPase (Rac1 or Rac2)[3–6]. Activation of NADPH oxidase is strictly regulated both temporally and spatially to ensure that the reaction takes place rapidly at the appropriate cellular localization. Activation of this system requires three signaling triggers, including protein kinases, lipid-metabolizing enzymes and nucleotide-exchange factors that activate the Rac GTPase[3–6].

Inadequate production of ROS is associated with various human pathological conditions. Deficiency of any component of the NADPH oxidase complex results in chronic granulomatous disease, in which bacterial and fungal infections are recurrent and life-threatening[4]. Abnormalities in the molecules involved in the signal-transduction pathway initiated by the recognition of pathogen-associated molecular patterns are accompanied by less production of ROS after exposure to specific stimuli and by susceptibility to bacterial infection. These abnormalities include deficiency in the kinase IRAK4, the adaptor MyD88 deficiency or the kinase NEMO (IKKγ)[7]. In contrast, many other human disorders are believed to be associated with or induced by excessive production of ROS that causes DNA damage, tissue damage, cellular apoptosis and neutropenia[8,9].

Here we focus on determining the role of the kinase Btk in production of ROS and cellular apoptosis in human neutrophils, as 11–30% of patients with X-linked agammaglobulinemia (XLA), a human disease of Btk deficiency, have neutropenia[10,11], and Btk is a critical signaling component of phagocytic cells[12–14]. The neutropenia of XLA is distinct from that of common variable immunodeficiency (CVID) in that the neutropenia is induced by infection, is usually ameliorated after supplementation with immunoglobulin and is not mediated by the autoimmune response[10,11,14]. Although a few reports have suggested that myeloid differentiation is impaired in mice with X-linked immunodeficiency[15,16], the reason for the infection-triggered neutropenia is unknown. The role of Btk in human neutrophils remains largely unexplored.

Btk is a member of the Tec-family kinases (TFKs) that are expressed in hematopoietic cells such as B cells, monocytes, macrophages and neutrophils[12]. It has a crucial role in cell survival, proliferation, differentiation and apoptosis, especially in cells of the B lineage. In humans with XLA, B cells fail to reach maturity and are presumably doomed to premature death by the *BTK* mutation that leads to the XLA phenotype[17]. Both mice with X-linked immunodeficiency that have natural mutations in *Btk* and mice in which *Btk* is targeted have B cell defects, but these are associated with much milder effects than those seen in XLA, which suggests species differences in the role of Btk[18,19].

[1]Department of Pediatrics and Developmental Biology, Tokyo Medical and Dental University Graduate School of Medical and Dental Sciences, Tokyo, Japan. [2]Department of Pediatrics, Teikyo University School of Medicine Hospital, Mizonokuchi, Kawasaki, Japan. [3]Department of Pediatrics, Toyama University School of Medicine, Toyama, Japan. [4]Department of Pediatrics, National Defense Medical College, Tokorozawa, Japan. [5]Department of Biotechnology, College of Life Science and Biotechnology, Yonsei University, Seoul, Republic of Korea. Correspondence should be addressed to T.M. (tmorio.ped@tmd.ac.jp).

Received 28 November 2011; accepted 12 January 2012; published online 26 February 2012; doi:10.1038/ni.2234

Btk is also an important signaling component of the innate immune system in phagocytic cells. Btk is involved in signaling via Toll-like receptors (TLRs) such as TLR2, TLR4, TLR7, TLR8 and TLR9, and is associated with the TLR adaptors MyD88, Mal (TIRAP) and IRAK1 (refs. 12–14,20–22). Defective innate immune responses have been observed in monocytes, dendritic cells, neutrophils and mast cells from Btk-deficient mice[12,14]. Neutrophils from mice with X-linked immunodeficiency have poor production of ROS and nitric oxide[15].

The contribution of Btk to the human innate immune system is less obvious. Stimulation via TLR2, TLR4, TLR7-TLR8 or TLR3 results in impaired production of tumor-necrosis factor (TNF) by dendritic cells from patients with XLA, whereas the TLR4-induced production of TNF and interleukin 6 (IL-6) by monocytes from patients with XLA remains intact[23–25]. Neutrophils from control subjects and patients with XLA show no substantial differences in their phosphorylation of the mitogen-activated protein kinases p38, Jnk and Erk induced by engagement of TLR4 or TLR7-TLR8 or production of ROS induced by the same stimuli[26].

Here we evaluate the role of Btk in the production of ROS and cellular apoptosis in human neutrophils through the use of Btk-deficient neutrophils, a protein-delivery system based on a cell-permeable peptide, and specific kinase inhibitors. Unexpectedly, and in contrast to published observations of mice with X-linked immunodeficiency[15], the production of ROS was substantially augmented in the absence of Btk in neutrophils stimulated via TLRs, the TNF receptor or phorbol 12-myristate 13-acetate (PMA) but not in monocytes or in lymphoblastoid B cell lines transformed by Epstein-Barr virus. Excessive production of ROS was associated with neutrophil apoptosis, which was reversed by the transduction of wild-type Btk protein. Btk-deficient neutrophils showed activation of key signaling molecules involved in the activation of NADPH oxidase, and this was accompanied by targeting of Rac2 to the plasma membrane. Mal was confined to the cytoplasm in association with Btk but was translocated to plasma membrane and interacted with protein tyrosine kinases (PTKs) and phosphatidylinositol-3-OH kinase (PI(3)K) in the absence of Btk. Here we present our findings on the mechanism by which Btk regulates the priming of neutrophils and the amplitude of the neutrophil response.

RESULTS

Excessive production of ROS in Btk-deficient neutrophils

To investigate the production of ROS in the absence of Btk, we monitored ROS in neutrophils, monocytes and Epstein-Barr virus–transformed lymphoblastoid B cell lines obtained from patients with XLA, healthy controls and patients with CVID (disease control) by staining with dihydrorhodamine 123 (DHR123) and a luminol chemiluminescence assay. PMA-driven production of ROS in Btk-deficient neutrophils was three to four times greater than that in neutrophils from healthy controls or patients with CVID, and we observed augmented production of ROS with a suboptimal dose of PMA, whereas the baseline production of ROS was similar (**Fig. 1a–d**). Similarly, and in contrast to published reports[26], engagement of TLR2 (with its ligand tripalmitoyl cysteinyl seryl tetralysine lipopeptide (Pam$_3$CSK$_4$)), TLR4 (with its ligand lipopolysaccharide) or the TNF receptor (with TNF) followed by stimulation with formyl-Met-Leu-Phe (fMLP), an agonist of G protein–coupled receptors, elicited augmented ROS responses in neutrophils from patients with XLA (**Fig. 1e,f**). The production of ROS was minimal after stimulation with the TLR9 agonist CpG-A in neutrophils from patients with XLA and was not significantly different from that of neutrophils from healthy controls. The observed phenomena were reproduced in Btk-deficient eosinophils but not in monocytes or Epstein-Barr virus–transformed lymphoblastoid B cell lines obtained from patients with XLA (**Supplementary Fig. 1**). These data indicated Btk-deficient neutrophils had excessive NADPH oxidase activity after various stimuli.

Augmented apoptosis in Btk-deficient neutrophils

Because high ROS concentrations are potentially harmful to cells, we investigated cell death induced by various stimuli in neutrophils from patients with XLA by staining with annexin V and the membrane-impermeable DNA-intercalating dye 7-AAD. Stimulation with PMA, TLR agonist plus fMLP, or TNF plus fMLP induced a significantly higher frequency of cells positive for annexin V among neutrophils from patients with XLA than among control neutrophils, whereas spontaneous cell death in the absence of stimulation was not significantly altered at 4 h in neutrophils from healthy controls versus those from patients with XLA (**Fig. 2a,b**). We observed cleavage of caspase-3, lower mitochondrial membrane potentials and degradation of proliferating

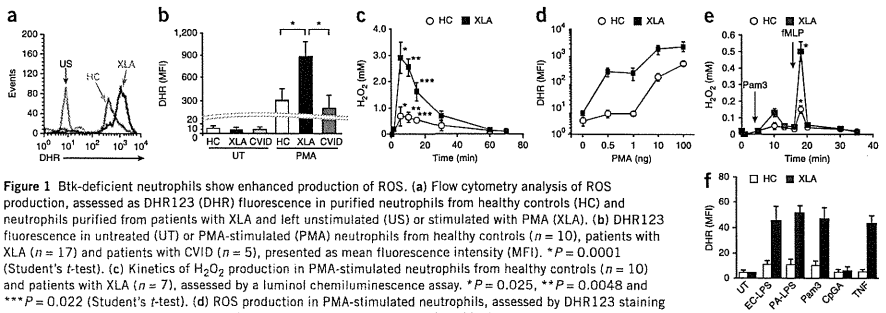

Figure 1 Btk-deficient neutrophils show enhanced production of ROS. (**a**) Flow cytometry analysis of ROS production, assessed as DHR123 (DHR) fluorescence in purified neutrophils from healthy controls (HC) and neutrophils purified from patients with XLA and left unstimulated (US) or stimulated with PMA (XLA). (**b**) DHR123 fluorescence in untreated (UT) or PMA-stimulated (PMA) neutrophils from healthy controls ($n = 10$), patients with XLA ($n = 17$) and patients with CVID ($n = 5$), presented as mean fluorescence intensity (MFI). $^*P = 0.0001$ (Student's t-test). (**c**) Kinetics of H_2O_2 production in PMA-stimulated neutrophils from healthy controls ($n = 10$) and patients with XLA ($n = 7$), assessed by a luminol chemiluminescence assay. $^*P = 0.025$, $^{**}P = 0.0048$ and $^{***}P = 0.022$ (Student's t-test). (**d**) ROS production in PMA-stimulated neutrophils, assessed by DHR123 staining and presented as a dose-response curve ($n = 5$ donors per group). (**e**) Kinetics of H_2O_2 production in neutrophils stimulated with Pam$_3$CSK$_4$ (Pam3) and fMLP, assessed by a luminol chemiluminescence assay ($n = 7$ donors per group). $^*P = 0.005$ (Student's t-test). (**f**) DHR123 fluorescence in neutrophils incubated with lipopolysaccharide from *Escherichia coli* (EC-LPS) or *Pseudomonas aeruginosa* (PA-LPS), Pam$_3$CSK$_4$, CpG-A or TNF, followed by stimulation with fMLP ($n = 7$ donors per group). Data are representative of seventeen experiments (**a**) or are pooled from at least five (**b,c,e,f**) or four (**d**) independent experiments (mean and s.d. in **b–f**).

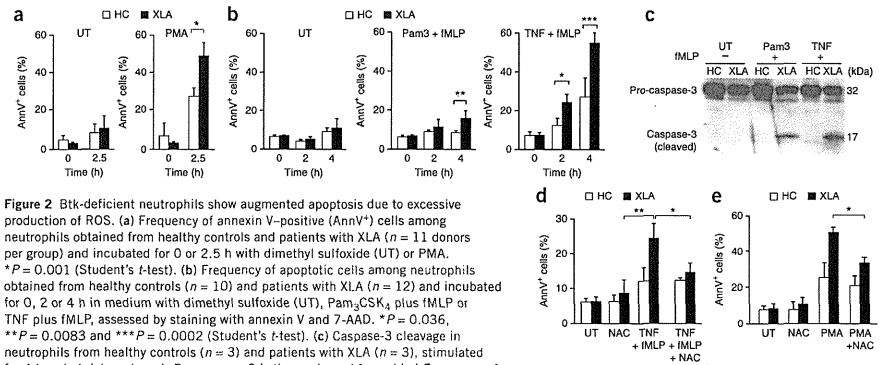

Figure 2 Btk-deficient neutrophils show augmented apoptosis due to excessive production of ROS. (**a**) Frequency of annexin V–positive ($AnnV^+$) cells among neutrophils obtained from healthy controls and patients with XLA ($n = 11$ donors per group) and incubated for 0 or 2.5 h with dimethyl sulfoxide (UT) or PMA. $^*P = 0.001$ (Student's *t*-test). (**b**) Frequency of apoptotic cells among neutrophils obtained from healthy controls ($n = 10$) and patients with XLA ($n = 12$) and incubated for 0, 2 or 4 h in medium with dimethyl sulfoxide (UT), Pam_3CSK_4 plus fMLP or TNF plus fMLP, assessed by staining with annexin V and 7-AAD. $^*P = 0.036$, $^{**}P = 0.0083$ and $^{***}P = 0.0002$ (Student's *t*-test). (**c**) Caspase-3 cleavage in neutrophils from healthy controls ($n = 3$) and patients with XLA ($n = 3$), stimulated for 4 h as in **b** (above lanes). Pro-caspase-3 is the uncleaved form. (**d**,**e**) Frequency of apoptotic Btk-deficient neutrophils ($n = 5$ donors) stimulated for 2 h (**d**) or 2.5 h (**e**) with the antioxidant N-acetyl-cysteine (NAC). $^*P = 0.043$ and $^{**}P = 0.036$ (**d**) or $^*P = 0.026$ (**e**; Student's *t*-test). Data are representative of three experiments (**b**) or at least five independent experiments (**a**,**c**–**e**; mean and s.d. in **a**,**b**,**d**,**e**).

cell nuclear antigen; hence, cell death was caused by apoptosis (**Fig. 2c** and **Supplementary Fig. 2**). Apoptosis assessed by these methods was augmented considerably for neutrophils from patients with XLA. The observed apoptosis was most probably triggered by ROS, as coincubation of neutrophils with N-acetyl cysteine, an antioxidant, rescued the cells from apoptosis induced by TNF plus fMLP or by PMA (**Fig. 2d,e**). We detected much more ROS release and stimulation-induced apoptosis of neutrophils from all patients with XLA regardless of the site or mode of their mutation (**Supplementary Fig. 3**). In addition, we found no correlation between genotype and the extent of neutrophil production of ROS. These data suggested that neutrophils from patients with XLA are susceptible to apoptosis triggered by pathogens.

Normalization of the ROS response by transduction of Btk

We next determined whether the enhanced apoptosis noted above was due to a defect in Btk itself or abnormal myeloid differentiation in the absence of Btk. For this, we prepared three recombinant Btk proteins (full-length Btk; Btk with deletion of the pleckstrin homology (PH) domain; and Btk with deletion of the kinase domain) fused to the cell-permeable peptide Hph-1 (**Fig. 3a,b**). We purified the products and transduced the proteins into neutrophils lacking Btk. The efficacy of transduction was more than 95%; and Hph-1–Btk expression was stable for at least 12–24 h (ref. 27). We adjusted the expression of Btk to that in neutrophils from healthy controls by incubating 1×10^6 cells for 1 h with 1 μM recombinant fusion protein. Transduction of full-length Btk into neutrophils from patients with XLA restored the production of ROS and the frequency of apoptotic cells after PMA stimulation to that observed for neutrophils from healthy controls (**Fig. 3c,d**). Transduction of the recombinant fusion of Btk with deletion of the PH domain only modestly reversed neutrophil overactivation (**Fig. 3c**), which indicated that appropriate cellular localization and interactions with other molecules were required for Btk function. Transduction of the recombinant fusion of Btk with deletion of the kinase domain minimally corrected excessive production of ROS (**Fig. 3c**), which suggested that the kinase activity of Btk or molecules that interacted via the kinase domain were critical for the regulation of ROS. We also confirmed the importance of the kinase domain by an experiment that showed excessive production of ROS in normal neutrophils treated with 50 μM LFM-A13, an inhibitor of the kinase activity of Btk, but not in those treated with LFM-A11, a control compound (**Fig. 3e**). We also documented augmented apoptosis in control neutrophils treated with LFM-A13 (**Fig. 3f**). These data demonstrated that the enhanced production of ROS and apoptosis was directly related to a defect in Btk.

NADPH oxidase components in Btk-deficient neutrophils

The NADPH oxidase complex consists of the transmembrane component ($gp91^{phox}$ and $p22^{phox}$), a cytosolic component ($p47^{phox}$, $p67^{phox}$ and $p40^{phox}$) and Rac2 (refs. 3–6). The activity of NADPH oxidase is controlled by targeting of the cytosolic components to the plasma membrane or phosphorylation of the cytosolic components or both. To assess the mechanism of the excessive production of ROS in Btk-deficient neutrophils, we investigated the abundance, phosphorylation and subcellular localization of each component by immunoblot analysis.

The expression of each component of the NADPH oxidase complex was similar in neutrophils from patients with XLA and those from healthy controls (**Fig. 4a**). The amount of $p47^{phox}$, $p67^{phox}$ and $p40^{phox}$ in the cytoplasm and the membrane was not substantially different in neutrophils from patients with XLA and those from healthy controls (**Fig. 4b**). Similarly, the amount in the membrane-targeted fraction after stimulation with PMA was not very different in neutrophils from patients with XLA and those from healthy controls (**Fig. 4c**). Phosphorylation of Ser345 in $p47^{phox}$ and of Thr154 in $p40^{phox}$ are important for translocation of the cytosolic components to the membrane[4,5,28]. Those modifications were not altered in Btk-deficient neutrophils (**Fig. 4c**). In contrast, we detected Rac2 in the plasma membrane of Btk-deficient neutrophils before stimulation with PMA. We observed four- to fivefold higher membrane expression of Rac2 in neutrophils from patients with XLA than in those from healthy controls in the resting state (**Fig. 4b**).

Typically, 10–15% of $gp91^{phox}$ is located in the plasma membrane of unstimulated neutrophils, whereas the majority of the molecule resides in specific granules. Membrane expression increases after

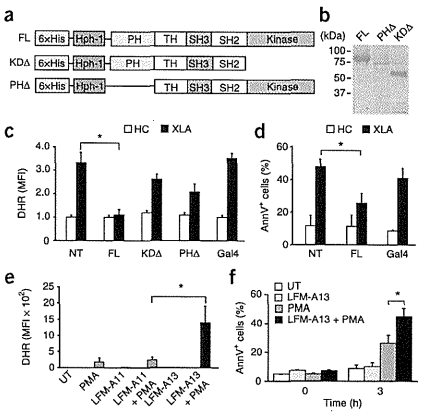

Figure 3 Excessive production of ROS and apoptosis in neutrophils from patients with XLA are abrogated by transduction of Hph-1–tagged full-length recombinant Btk but not by Hph-1–tagged Btk with deletion of the kinase or PH domain. (**a**) Hph-1–tagged Btk constructs: full-length Btk (FL); Btk with deletion of the kinase domain (KDΔ); Btk with deletion of the PH domain (PHΔ). 6xHis, six-histidine tag; TH, Tec homology; SH3, Src homology 3; SH2, Src homology 2. (**b**) Size of purified Hph-1–tagged Btk proteins, confirmed by Coomassie brilliant blue staining. (**c**) ROS production in neutrophils from healthy controls ($n = 5$) and patients with XLA ($n = 5$), left untransduced (NT) or transduced with the constructs in **a** or Hph-1–tagged yeast transcriptional activator Gal4 (far right; control), presented as the MFI of DHR123 relative to that of untreated neutrophils from healthy controls, set as 1. (**d**) Frequency of apoptotic cells among neutrophils from healthy controls and patients with XLA, left untransduced or transduced with Hph-1–tagged full-length Btk or Gal4 (control). (**e**) DHR123 fluorescence in neutrophils from healthy controls ($n = 7$) left untreated or treated with PMA alone, or pretreated with LFM-A13 (Btk inhibitor) or LFM-A11 (control) alone or followed by stimulation with PMA (+ PMA). (**f**) Frequency of annexin V–positive cells among neutrophils from healthy controls ($n = 7$) left untreated or treated with PMA alone, or pretreated with LFM-A13 (50 μM, a concentration that does not inhibit other PTKs[47,48]) alone or followed by stimulation with PMA. $^*P = 0.0021$ (**c**), 0.019 (**d**), 0.021 (**e**) or 0.025 (**f**; Student's *t*-test). Data are representative of five experiments (**b**) or are pooled from six (**c**), three (**d**) or four (**e**,**f**) independent experiments (mean and s.d. in **c**–**f**).

signaling via TLRs or G protein–coupled receptors because of translocation to the plasma membrane[2]. Immunoblot analysis with antibody to gp91 (anti-gp91; **Fig. 4b**) and flow cytometry analysis of surface flavocytochrome b_{558} (**Fig. 4d**) showed higher gp91 expression in neutrophils from patients with XLA. Immunohistochemical analysis by confocal fluorescence microscopy showed localization of gp91 and Rac2 together in the membranes of resting Btk-deficient neutrophils but not in neutrophils from healthy controls (**Fig. 4e**). These results suggested that NADPH oxidase complex was partially assembled and ready to be activated in steady-state Btk-deficient neutrophils.

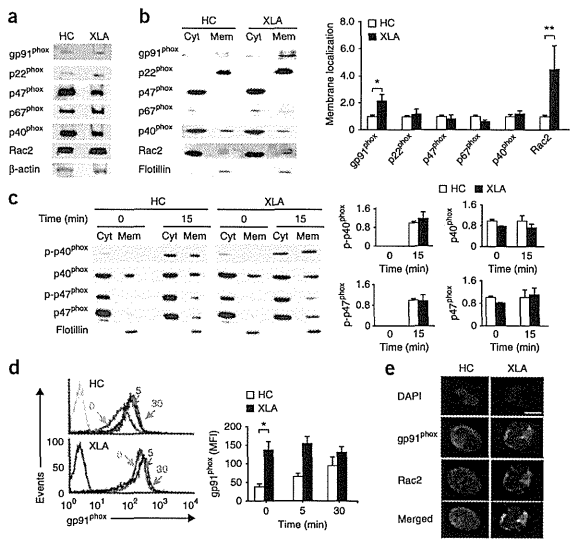

Figure 4 Btk-deficient neutrophils show targeting of Rac2 to the plasma membrane, colocalization of Rac2 with $gp91^{phox}$ and higher membrane expression of $gp91^{phox}$. (**a**) Immunoblot analysis of the components of the NADPH oxidase complex in neutrophils from a healthy control and a patient with XLA. β-actin serves as a loading control throughout. (**b**) Immunoblot analysis (left) of the components of the NADPH oxidase complex in the cytoplasm (Cyt) and plasma membrane (Mem) of neutrophils from healthy controls and patients with XLA ($n = 9$ per group). Right, quantification of the membrane expression at left, presented as band intensity relative to that of flotillin (loading marker for the membrane-raft fraction) in membranes of neutrophils from healthy controls, set as 1. $^*P = 0.045$ and $^{**}P = 0.027$ (Student's *t*-test). (**c**) Immunoblot analysis of total and phosphorylated (p-) $p40^{phox}$ and $p47^{phox}$ in the cytoplasm and membrane of PMA-stimulated neutrophils from healthy controls and patients with XLA. Right, quantification as in **b**. (**d**) Flow cytometry analysis of $gp91^{phox}$ on neutrophils from healthy controls and patients with XLA, left unstimulated (0) or stimulated for 5 or 30 min (above lines) with PMA, detected by staining with mAb 7D5 to gp91. Gray lines indicate staining with MsIgG (control). Right, quantification of the gp91 MFI in cells treated as at left. $^*P = 0.0039$ (Student's *t*-test). (**e**) Confocal microscopy of $gp91^{phox}$ (green) and Rac2 (red) in healthy controls and neutrophils from patients with XLA; nuclei are counterstained with the DNA-intercalating dye DAPI (blue). Original magnification, ×600; scale bar, 10 μm. Data are from one representative of nine independent experiments with seven healthy controls and nine patients with XLA (**a**), are representative of nine experiments (**b**), are from nine independent experiments (**c**), are pooled from seven independent experiments (**d**) or are representative of four independent experiments (**e**; mean and s.d. in **b**–**d**).

Activated PTKs and PI(3)K in resting XLA neutrophils

Assembly and activation of the cytosolic components and Rac requires the involvement of kinases such as PTKs, PI(3)K and protein kinase C. We thus explored a potential signaling pathway that would lead to the partial assembly of NADPH oxidase. First, we examined the extent of tyrosine phosphorylation of cellular substrates in Btk-deficient and Btk-sufficient neutrophils before and after stimulation with PMA. Btk-deficient neutrophils showed hyperphosphorylation of protein species in the range of 50–53 kilodaltons (kDa), 72 kDa, 85 kDa and 150 kDa at baseline relative to phosphorylation in neutrophils from healthy controls (**Fig. 5a**). TLR4-mediated stimulation led to more phosphorylation of protein species 38 kDa, 50–53 kDa, 60 kDa, 72 kDa and 85 kDa in size in Btk-deficient neutrophils (**Supplementary Fig. 4a**).

In contrast, the baseline PTK activity in monocytes from patients with XLA was unaltered or slightly diminished relative to that of monocytes from healthy controls. TLR2-stimulated activation of PTKs was largely similar or slightly less in the absence of Btk (**Supplementary Fig. 4b**). We were able to directly ascribe the enhanced PTK activity to the absence of Btk, as transduction of recombinant Btk into neutrophils from patients with XLA restored baseline phosphorylation to that seen in neutrophils from healthy controls (**Fig. 5b**).

We next searched for tyrosine-phosphorylated proteins in Btk-deficient neutrophils through the use of phosphorylation-specific antibodies. The expression and activation of Tec and Bmx, TFKs present in neutrophils, was not upregulated in neutrophils from patients with XLA (**Fig. 5c**), which indicated that they did not compensate for Btk function. However, we found that the tyrosine-phosphorylated proteins 50–53 kDa, 72 kDa, 85 kDa and 150 kDa in size were the kinases Lyn and c-Src, Syk, the p85 subunit of PI(3)K (class IA) and FAK, respectively (**Fig. 5d,e**). We found that c-Src, Syk, PI(3)K-p85 and FAK were phosphorylated at their tyrosine residues that have a positive regulatory function. Notably, Lyn, a kinase known to have positive as well as negative roles in the modulation of myeloid function, was phosphorylated at Tyr507, a negative regulatory site[29–31].

We first focused on PI(3)K, as PI(3)K activation targets Rac2 to flavocytochrome b_{558}; this process is important for converting

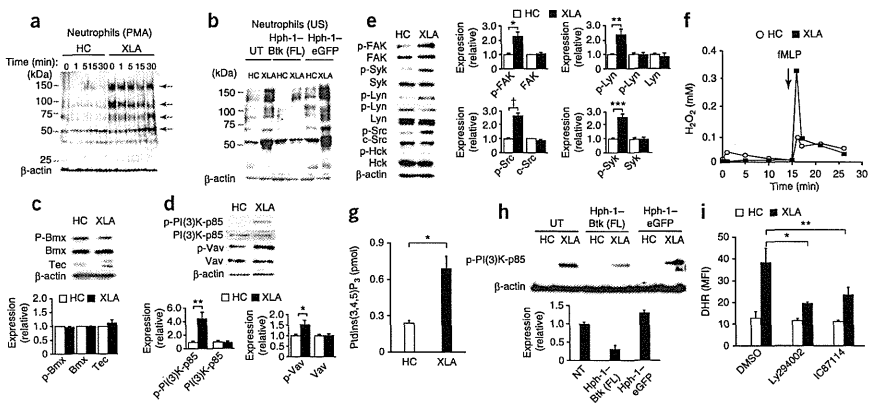

Figure 5 Btk-deficient neutrophils have higher baseline activity of PTKs and PI(3)K, which is reversed by transduction of recombinant Btk protein. (**a**) Immunoblot analysis of phosphorylated tyrosine in lysates of PMA-stimulated neutrophils from healthy controls ($n = 5$) and patients with XLA ($n = 7$). Arrows indicate hyperphosphorylated proteins in neutrophils from patients with XLA at 0 min. (**b**) Immunoblot analysis of phosphorylated tyrosine (as in **a**) in lysates from unstimulated (US) neutrophils from healthy controls ($n = 4$) and patients with XLA ($n = 5$), left untransduced or transduced with Hph-1–tagged full-length Btk or eGFP. (**c**,**d**) Immunoblot analysis (top) of whole-cell lysates of neutrophils from healthy controls ($n = 5$) and patients with XLA ($n = 7$), probed for total and phosphorylated Bmx and total Tec (**c**) or total and phosphorylated PI(3)K-p85 and Vav (phosphorylated at Tyr508 (PI(3)K-p85) or Tyr174 (Vav); d). Phosphorylated Tec was not detected by immunoblot analysis of phosphorylated tyrosine in samples immunoprecipitated with anti-Tec (data not shown). Bottom, quantification of the expression at top, presented relative to expression of β-actin in neutrophils from healthy controls, set as 1. $*P = 0.038$ and $**P = 0.0001$ (Student's *t*-test). (**e**) Immunoblot analysis (left) of neutrophils from healthy controls ($n = 5$) and patients with XLA ($n = 7$), probed for total PTKs and PTKs phosphorylated at Tyr576 and Tyr577 (FAK); Tyr524 and Tyr525 (Syk); Tyr507 (Lyn; top) or Tyr397 (Lyn; bottom); (Tyr416 (c-Src); and Tyr411 (the kinase Hck). Phosphorylated PTKs Fgr and Yes were undetectable (data not shown). Right, quantification as in **c**,**d**. $*P = 0.033$, $**P = 0.004$, $***P = 0.0007$ and $\dagger P = 0.0002$ (Student's *t*-test). (**f**) H_2O_2 production by fMLP-stimulated neutrophils from healthy controls and patients with XLA ($n = 5$ per group). (**g**) Enzyme-linked immunosorbent assay of phosphatidylinositol-(3,4,5)-trisphosphate (PtdIns(3,4,5)P_3) in unstimulated neutrophils from patients with XLA ($n = 5$). $*P = 0.0005$ (Student's *t*-test). (**h**) Immunoblot analysis (top) of phosphorylated PI(3)K-p85 in neutrophils from healthy controls and patients with XLA ($n = 5$ per group), left untransduced or transduced with Hph-1–tagged full-length Btk or eGFP. Detection of phosphorylated PI(3)K-p85 in neutrophils from healthy controls required longer exposure. Below, quantification of results above, presented relative to the expression of phosphorylated PI(3)K-p85 relative to that of β-actin in neutrophils from patients with XLA, set as 1. (**i**) Production of ROS in neutrophils from patients with XLA, treated with dimethyl sulfoxide (DMSO) or preincubated with Ly294002 (universal PI(3)K inhibitor; 50 μM)[32] or IC87114 (PI(3)Kδ inhibitor; 1 μM (a concentration that does not inhibit PI(3)Kα, PI(3)Kβ or PI(3)Kγ)[33]) and stimulated with fMLP. $*P = 0.006$ and $**P = 0.003$ (Student's *t*-test). Data are representative of or pooled from six (**a**,**f**), seven (**b**–**e**), four (**g**), eight (**h**) or five (**i**) independent experiments (mean and s.d. in **c**–**e**,**g**–**i**).

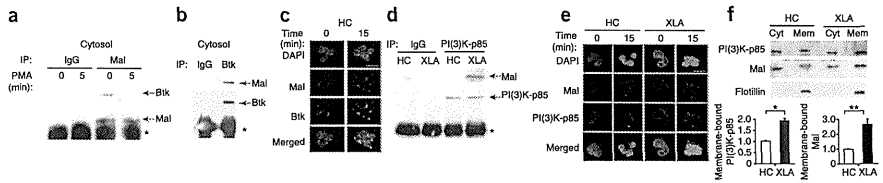

Figure 6 Mal in neutrophils from healthy controls associates with Btk in the resting state and translocates to the plasma membrane after stimulation, whereas Mal associates with PI(3)K at the plasma membrane in Btk-deficient neutrophils. (**a**,**b**) Coimmunoprecipitation analysis of Btk and Mal in the cytoplasmic fraction of neutrophils from healthy controls, left unstimulated (0 (**a**), b) or stimulated for 5 min with PMA (5 (**a**)). IP, immunoprecipitation; IgG, control antibody. *, immunoglobulin light chain (**a**) or heavy chain (**b**). (**c**) Confocal microscopy of neutrophils from healthy controls, left unstimulated (0) or stimulated for 15 min with PMA (15), then stained with anti-Mal (red) and anti-Btk (green) and counterstained with DAPI. Original magnification, ×600; scale bar, 10 μm. (**d**) Coprecipitation analysis of PI(3)K-p85 and Mal in membrane fraction of neutrophils from healthy controls and patients with XLA. *, immunoglobulin heavy chain. (**e**) Confocal microscopy of neutrophils from healthy controls and patients with XLA, left unstimulated or stimulated for 15 min with PMA, then stained with anti-Mal (red) and anti-PI(3)K-p85 (green) and counterstained with DAPI. Scale bar, 10 μm. (**f**) Immunoblot analysis (above) of PI(3)K-p85 and Mal in the cytoplasm and plasma membrane of unstimulated neutrophils from healthy controls and patients with XLA. Below, quantification of results above, presented relative to the expression of flotillin in neutrophils from healthy controls, set as 1. $*P = 0.0035$ and $**P = 0.0021$ (Student's *t*-test). Data are representative of three (**a**,**b**), four (**c**,**e**), six (**d**) or seven (**f**) independent experiments (mean and s.d. in **f**).

neutrophils into a 'primed' state in which they are ready for complete activation of NADPH oxidase triggered by stimuli such as fMLP. Indeed, Btk-deficient neutrophils were in a primed state, as fMLP alone elicited excessive production of ROS (**Fig. 5f**). Greater phosphorylation of PI(3)K-p85 was accompanied by more enzymatic activity, as shown by more baseline production of phosphatidylinositol-(3,4,5)-trisphosphate and by phosphorylation of the adaptor Vav (**Fig. 5d**,g). Furthermore, augmented PI(3)K activation was normalized, although only partially, by transduction of full-length Btk linked to Hph-1 (**Fig. 5h**).

The importance of PI(3)K in inducing the primed state was supported by data showing inhibition of fMLP-driven production of ROS by preincubation of Btk-deficient neutrophils with the universal PI(3)K inhibitor LY294002 at a concentration of 50 μM (refs. 32,33). We observed this inhibition in cells incubated with the PI(3)Kδ–specific inhibitor IC87114 at a concentration of 1 μM (ref. 33) but not in those incubated with the PI(3)Kγ–specific inhibitor AS605240 at a concentration of 8 nM (ref. 34; **Fig. 5i** and **Supplementary Fig. 5a**). These findings suggested PI(3)Kδ activation was involved in the excessive ROS response.

Interaction of membrane-targeted Mal with PI(3)K

We next sought the reason for the PI(3)K activation in the absence of Btk. For this, we first focused on a molecule that interacts with both Btk and PI(3)K. Evidence obtained with monocytes indicates that Mal is a critical component of TLR2-TLR4 signaling and is a target of Btk[13,14,20,21]. The TLR signal triggers activation of Btk, which in turn phosphorylates Mal. Phosphorylated Mal translocates to the plasma membrane via phosphatidylinositol-(4,5)-bisphosphate (PtdIns(4,5)P_2) and then interacts with and activates PI(3)K[35].

Unexpectedly, coimmunoprecipitation assays of neutrophils from human controls demonstrated that Mal was associated with Btk in the resting state (**Fig. 6a**,**b**). We observed colocalization of Mal and Btk in the cytoplasm and, after activation of cells with PMA, we detected the Mal-Btk complex at the membrane by immunofluorescence staining (**Fig. 6c**).

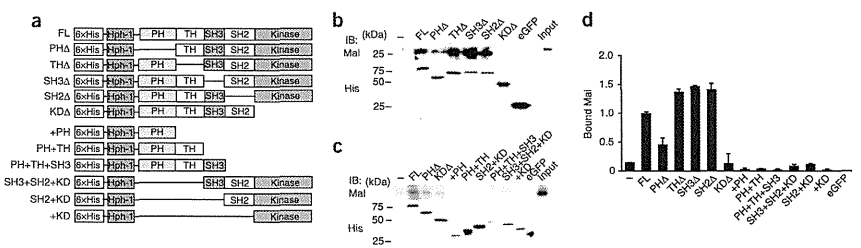

Figure 7 Btk associates with Mal at the PH and kinase domains. (**a**) Hph-1–tagged Btk constructs: full-length Btk (FL); Btk mutants with deletion of the PH domain (PHΔ), Tec homology (THΔ), SH3 domain (SH3Δ), SH2 domain (SH2Δ) or kinase domain (KDΔ); and Btk mutants with truncation retaining (+) only some domains (bottom six). (**b**,**c**) Immunoblot analysis (IB) of Mal (top) in extracts of cytoplasm of neutrophils from healthy controls, incubated with nickel beads bound to Hph-1–tagged recombinant full-length Btk or the deletion mutants (**b**) or truncation mutants (**c**) in **a**, or to Hph-1–tagged eGFP (negative control). Below, immunoblot analysis after rebinding to nickel beads, probed with anti-histidine (His). To make these as equimolar as possible, more beads were added for the +PH, PH+TH+SH3, SH3+SH2+KD and +KD constructs. Input, cytoplasmic extracts without precipitation. (**d**) Quantification of Mal bound to the recombinant Btk proteins based on the results in **b**,**c** ($n = 4$ donors), presented to results for full-length Btk, set as 1. Data are representative of four experiments (**b**,**c**) or are a summary of four independent experiments (**d**; mean and s.d.).